Horizon Europe programme, grant agreement No. 101096068S

RETROFIT SOLUTIONS TO ACHIEVE 55% GHG REDUCTION BY 2030

Definition of retrofitting options based on combination of different alternatives

WP 6 – Electrification and energy management of on-board systems
Task 6.2 – Investigating the retrofitting of zero-carbon solutions
D6.4 – Definition of retrofitting options based on combination of different alternatives
Partners involved: LJMU, CNR, NTUA, RINA, ATD
Authors: Onur Yuksel (LJMU), G Viknash Shagar (LJMU), Eduardo Blanco-Davis (LJMU), Andrew Spiteri (LJMU), David Hitchmough (LJMU), Jin Wang (LJMU), Maria Carmela di Piazza (CNR), Marcello Pucci (CNR), Giulio Rodonò (CNR), John Prousalidis (NTUA), Elias Sofras (NTUA), Nikos Themelis (NTUA).

Project details

Project Title	RETROFIT SOLUTIONS TO ACHIEVE 55% GHG REDUCTION BY 2030
Project Type	Innovation Action
Project Acronym	RETROFIT55
Grant Agreement No.	101096068
Duration	36 M
Project Start Date	01/01/2023

Deliverable information

Status (F: final; D: draft; RD: revised draft)	D
Planned delivery date	31/03/2025
Actual delivery date	14/04/2025
• **Dissemination level:** PU – Public, fully open, e.g., web (Deliverables flagged as public will be automatically published in CORDIS project's page) • SEN – Sensitive, limited under the conditions of the Grant Agreement • Classified R-UE/EU-R – EU RESTRICTED under the Commission Decision No2015/444 • Classified C-UE/EU-C – EU CONFIDENTIAL under the Commission Decision No2015/444 Classified S-UE/EU-S – EU SECRET under the Commission Decision No2015/444	PU
Type: Report, Website, Other, Ethics	Report

Document history

Version	Date	Created/Amended by	Changes
01	02/12/2024	Onur Yuksel (LJMU) Viknash Shagar (LJMU)	First draft
02	27/03/2025	Onur Yuksel (LJMU) Viknash Shagar (LJMU)	Second draft
03	08/04/2025	Maria Carmela Di Piazza Marcello Pucci	Third Draft/ Technical Revisions
04	14/04/2025	Onur Yuksel (LJMU) Viknash Shagar (LJMU)	Final version

Quality check review

Reviewer (s)	Main changes / Actions
Marcello Pucci, Maria Carmela Di Piazza (CNR)	Review of the document, technical comments and suggestions.
Cecilia Leotardi (CNR)	Editorial review.
Cecilia Leotardi & Alessandro Iafrati (CNR)	Final review of contents and submission to EC.

Table of Contents

List of figures

List of tables

List of abbreviations

Abbreviation	Definition	Unit
BOP	Balance of Plant	-
C_B	Available Battery Capacity	kWh
C_E	Emission Coefficient for Fuel Cells	g/kWh
C_i	Initial Capacity	kWh
$C_{p,ex}$	Heat Capacity of the Exhaust	kJ/kg
CC-CV	Constant Current Constant Voltage	-
CFE	Constant Frequency Electrical	-
CH_4	Methane	-
CO_2	Carbon dioxide	-
$CO_{2\text{-}eq}$	Equivalent Carbon dioxide	-
CII	Carbon Intensity Indicator	-
D-MPPT	Distributed Maximum Power Point Tracking	-
D/G	Diesel Generator	-
DMG	Direct Mounted Generator	-
e^-	Electrons	-
EEDI	Energy Efficiency Design Index	-
EEXI	Energy Efficiency Existing Index	-
EMS	Energy Management Strategy	-
ESS	Energy Storage System	-
FC	Fuel Cell	-
G	Instantaneous Value of Solar Radiation on the Panel	W/m^2
H^+	Hydrogen Protons	-
H_2O	Water	-
H_3PO_4	Liquid Phosphoric Acid	-
I_B	Battery Current	A
I_{PEMFC}	PEMFC current	A
ICE	Internal Combustion Engine	-
IMO	International Maritime Organization	-
GHG	Greenhouse Gas	-
GCR	Gear Constant Ratio	-

GWP	Global Warming Potential	-
LNG	Liquefied Natural Gas	-
LT	Lifespan	hours or years
M/E	Main Engine	-
MARPOL	The International Convention for the Prevention of Pollution from Ships	-
MCFC	Molten Carbonate Fuel Cell	-
MCR	Maximum Continuous Rate	-
MPPT	Maximum Power Point Tracker	-
N_2O	Nitrous Oxide (Dinitrogen Oxide or Dinitrogen Monoxide)	-
n_{FC}	Number of Active Fuel Cells	-
NOCT	The Operating Cell Temperature under G=800 W/m^2	°C
NOx	Nitrogen Oxides	-
O_2	Oxygen	-
ORC	Organic Rankine Cycles	-
PAFC	Phosphoric Acid Fuel Cell	-
P	Power Output	kW
P_B	Battery Power	kW
P_{inv}	Inverter Power	kW
P_{PV}	Photovoltaic Power	kW
PEMFC	Proton Exchange Membrane Fuel Cell	-
PM	Particulate Matter	-
PTH	Power-Take-Home	-
PTI	Power-Take-in	-
PTO	Power-Take-off	-
PV	Photovoltaic	-
RCF	Resonant Constant Frequency	-
S	Surface of the PV field	-
SFOC	Specific Fuel Oil Consumption	-
SOx	Sulphur Oxides	-
SoC	State of Charge	-
SoH	State of Health	-
SOFC	Solid Oxide Fuel Cell	-

SMG	Shaft Mounted Generator	-
t	Operation Time	hours
T_e	Ambient Temperature	°C
T_{cell}	PV Cell Temperature	°C
$T_{in, ex}$	ORC Evaporator Inlet Temperature	°C or °K
$T_{out, ex}$	ORC Evaporator Outlet Temperature	°C or °K
WHRS	Waste Heat Recovery System	-
V_{Grid}	Ship grid voltage	V
VFD	Variable Frequency Drive	-
VOC	Volatile Organic Compounds	-
Greek Letters		
η_{act}	Actual Efficiency	-
η_C	Columbic Efficiency	-
η_i	Initial Efficiency	-
η_{inv}	Inverter Conversion Efficiency	-
η_{ORC}	ORC Efficiency	-
η_{PC}	Power Converter Efficiency	-
η_{PV}	PV Efficiency	-

Executive Summary

The maritime industry is moving decisively toward full decarbonisation, driven by the need to mitigate environmental impact and align with global sustainability goals. The primary focus is on the transition to renewable energy sources and zero-carbon fuels, particularly hydrogen and ammonia. Extensive research and real-world applications have already illustrated the feasibility of adopting hydrogen-rich fuels—such as liquefied natural gas (LNG) and methanol—for marine use, especially in conjunction with fuel cell (FC) technologies. However, the diversity of hydrogen-rich fuels and the range of power generation technologies available make a single, standardised solution unfeasible. Instead, the optimal selection of a power plant must be tailored to the specific type of ship and its operational profile, considering whether internal combustion engines or FCs provide the most suitable option. This careful customisation is essential to maximise greenhouse gas reductions for long-distance navigation and to address emissions during port operations.

One of the critical areas of exploration involves combining FCs and batteries to enhance energy efficiency indicated in Chapter 2. Current FC technology faces challenges in adapting to fluctuating power demands, necessitating a hybrid approach that incorporates small-scale battery storage. This integration is designed to stabilise energy output and increase overall efficiency, protecting the power system from wear and optimising generator performance. Assessments use indicators such as fuel consumption and emissions to identify best practices. Additionally, there is a need to analyse the supporting machinery required for fuel handling, bunkering, and delivery, with the aim of configuring the most effective engine room layout.

Energy optimisation efforts extend to enhancing the performance of main propulsion systems. A key strategy includes the use of a variable-speed shaft generator system demonstrated in Chapter 3, which can provide flexibility in energy management. The system can supply energy to the ship's electric grid or an energy storage unit, and alternatively, it can function as a propulsion booster to improve the ship's efficiency and reduce its environmental impact. These innovations aim to achieve a more sustainable energy profile for the maritime sector.

The integration of renewable energy sources, particularly through photovoltaic (PV) technology depicted in Chapter 4, is another significant aspect of the decarbonisation strategy. The feasibility of using solar energy has been evaluated according to ship type and specific operational needs. These design studies are geared towards meeting emission reduction goals and enhancing the energy efficiency of maritime operations.

The comprehensive approach to decarbonising the shipping industry requires a combination of innovative solutions, hybrid energy systems, and renewable energy technologies. This multifaceted strategy acknowledges the diversity of maritime operations and seeks to tailor solutions that optimise environmental performance while maintaining the functionality and economic viability of the fleet.

1 Introduction

Global warming, driven by increasing levels of greenhouse gases (GHG) in the atmosphere, is one of the most urgent global challenges we face today [1]. The surge in extreme weather events has drawn more attention to this issue in recent years [2]. Although shipping is the most efficient mode of transporting goods, it significantly contributes to global warming and air pollution due to the widespread use of heavy marine fuels and its extensive capacity [3]. Maritime transport accounts for 3% of global GHG emissions, including carbon dioxide (CO2), nitrous oxide (N2O), and methane (CH4) [4]. Besides GHGs, shipping also emits particulate matter (PM), volatile organic compounds (VOCs), sulphur oxides (SOx), and nitrogen oxides (NOx) [5]. These pollutants not only drive global warming but also pose serious health risks, especially in coastal regions where air pollution from maritime activities is more concentrated [6].

In response to these environmental concerns, the International Maritime Organization (IMO) updated its targets in 2023 to further reduce the carbon footprint of the shipping industry [7]. The revised goals aim for a 20% reduction in emissions by 2030, a 70% reduction by 2040 compared to 2008 levels, and achieving net-zero emissions by 2050 [8]. To meet these targets, the IMO introduced the Energy Efficiency Existing Ship Index (EEXI) and the Carbon Intensity Indicator (CII) to steer the global fleet toward greater sustainability. To comply with these new standards, a variety of measures can be implemented onboard ships. These include optimising traditional systems through engine power limitations, hull cleaning, air lubrication, the use of energy-saving devices, and route or speed optimisation to improve energy efficiency [9]. For deeper emission cuts, especially to meet the 2040 and 2050 targets, ships may adopt Photovoltaic (PV) panels, wind systems, batteries, inverter fed electrical drives for pumps and compressors on board, Power Take Off (PTO) / Power Take In (PTI) systems, waste heat recovery systems (WHRS), or retrofit to alternative fuels and technologies that replace or complement traditional internal combustion engines (ICEs) [10].

Renewable energy-based designs targeting marine power distribution systems are particularly suitable for early applications on large maritime vessels due to the lower and more steady power demands of ship electrification system compared to the main propulsion plant [11]. Hybrid FC configurations are especially recommended for reducing maritime emissions, as they are adaptable to alternative fuels such as liquefied natural gas (LNG), ammonia, or hydrogen (H_2). These systems offer advantages like high modularity, efficiency, low air and noise emissions, the absence of moving parts, and reduced maintenance needs [12]. Moreover, they are not well-suited for handling rapid load variations and are typically paired with batteries to mitigate this limitation [13]. As a result, their application in large marine propulsion systems can be challenging. However, they are more viable for use in power generation plants focused on electrification [14].

Currently, commercially available FC technologies for power applications include proton exchange membrane FCs (PEMFCs), alkaline FCs, direct methanol FCs, phosphoric acid FCs (PAFCs), molten carbonate FCs (MCFCs), and solid oxide FCs (SOFCs). High-temperature FCs, such as MCFC or SOFC have the advantage of enabling integrated fuel reforming, allowing them to produce H2 directly from LNG or ammonia [15]. However, their elevated operating temperatures also lead to slower start-up times and greater operational constraints [16]. PEMFCs stand out due to their high electrical efficiency and advanced technological development [17]. Their shorter start-up time makes them particularly suitable for transportation applications [18]. However, they require high-purity hydrogen, which complicates their operation on ships [19]. Current FC technology encounters challenges in adapting to fluctuating power demands, making a hybrid approach including a battery storage essential. This integration aims to stabilise energy output, enhance overall efficiency, protect the power system from excessive wear, and optimise the plant performance [20]. Evaluations rely on metrics such as fuel consumption and emissions to determine best practices. Furthermore, there is a need to assess the auxiliary machinery required for fuel handling, bunkering, and delivery, with the goal of designing the most efficient engine room layout [21].

WHRS can reduce waterborne GHG emissions by enhancing overall fuel energy efficiency. In large two-stroke diesel engines only about 50% of fuel is converted to mechanical energy, while the other 50% is lost as waste heat through exhaust gases, cooling fluids, and thermal radiation. Similar efficiency levels are expected for future engines using green fuels like methanol, indicating that WHRS will remain relevant even if the maritime sector fully transitions to sustainable fuels [22]. Organic Rankine Cycle (ORC) systems have been identified as an effective technology for recovering low-grade waste heat from ships. In recent years, ORC installations have begun to be implemented, primarily utilising waste heat from jacket water and exhaust gases [23]. ORC systems can convert waste heat from machinery into mechanical or electrical energy. This energy can be utilised for additional propulsion power or to meet utility service demands, reducing fuel consumption and CO_2 emissions [10, 24].

PTO and PTI systems, commonly called shaft generators, have been integrated on vessels as retrofit solutions. These systems leverage the efficiency of the M/E for electrical power generation, known as PTO, with conventional diesel engine generators. Alternatively, they function as supplementary motors to enhance propulsion power, referred to as PTI. This integration allows for the incorporation of energy storage solutions, shore-to-ship power, and other innovative energy sources within the power and propulsion framework. During navigation, the PTI/PTO approach effectively addresses electrical demands with improved efficiency [25]. Key advantages of PTO/PTI technologies include reduced fuel consumption and emissions, enhanced operational flexibility, and lower maintenance costs due to diminished reliance on separate auxiliary generators. However, it is important to note that these systems do not generate electrical power while in port and below certain ship speeds and may increase the load on the M/E, potentially leading it to instability, if not properly dimensioned. Overall, PTO/PTI technologies represent a significant advancement in hybrid propulsion systems, optimising energy efficiency and operational performance [26].

Another prominent candidate for supporting ship electrification has been PV panels, with their application onboard dating back as far as 50 years. The applications of PV modules in shipping have primarily involved supplying electric energy to motors used for propulsion in smaller recreational and mainly inland watercraft. These vessels share common characteristics: smaller dimensions, stable operation without rolling motion, and low service speeds, leading to minimal propulsion power requirements. PV installations have also been, and continue to be, used on larger ships, but primarily for charging batteries that power lighting and other electrical systems [27]. Although to date the use of on-board PV systems has been limited, due to the need for large surfaces and high capital costs, the IMO GHG strategy for 2050 is currently pushing stakeholders in the shipping industry to explore the integration of on-board PV systems as a practical solution to reduce fuel consumption and pollutant emissions[28]. Particularly, PV applications on cargo ships are growing [29, 30], supported by research projects suggesting PV ship integration as a promising solution for assisting/relieving auxiliary power generation from diesel gensets, thus reducing fuel consumption and polluting emissions, [31, 32].One of the key factors to be considered is the selection of most suitable ships for PV integration; by this standpoint, bulk carriers, with their large main deck areas, are particularly well-suited for PV integration. Key challenges for wider adoption include the assessment of economic viability, optimising PV integration into ship power systems, and refining installation and operation issues.

1.1 Aims and Objectives

This report aims to provide a comprehensive series of numerical analyses on technologies for retrofitting ship electrification systems to reduce fuel consumption and resulting emissions. This report aims to establish a framework for evaluating environmental benefits and onboard settlement-related factors, offering insights into current challenges, regulatory frameworks, and potential solutions through the perspective of the Poseidon Principles, European Union, and IMO requirements.

The objectives to achieve the aim have been determined as:

- To develop a simulation framework for assessing the suitability of different FC types (PAFC, PEMFC, and SOFC) in combination with batteries and WHRS using a scenario-based approach.
- To generate electrical energy on-board by integrating a shaft generator system that optimises the main engine's operating point. The system can integrate an energy management, acting on the proper charge or discharge of a storage system. During PTI operation, it can also boost the main propulsion engine, enhancing energy efficiency and reducing the ship's environmental footprint or permitting safe return-to-port.
- To assess the utilisation of PV panels into the ship's electrification system for evaluating the potential for emission reduction. To explore the designs involving traditional and novice technologies such as flexible PV panels.

1.2 Report Structure

This report is divided into five chapters, including this introductory chapter, which provides an overview of the background, aims, and objectives.

- Chapter 2 focuses on the evaluation of FCs, batteries, and WHRS within the ship's electrification system. It presents a detailed presentation of various power configurations utilising these technologies, explains the working principles of each power system, and outlines the mathematical foundations and modelling logic.
- Chapter 3 explores the application of PTO/PTI systems on marine vessels, examining potential outcomes from their integration into ship electrification and propulsion.
- Chapter 4 covers the assessment of PV panel technologies integration within the power distribution system of the case study vessel.
- Chapter 5 concludes the report, summarising the findings and work conducted within this framework.

1.3 Case Study Vessel

This study utilises data gathered from the bulk carrier M/V KASTOR, which is owned and managed by the project partner, LASKARIDIS SHIPPING CO., LTD. The data collection period spanned from February 1, 2021, to February 10, 2023, with a sampling interval of one minute. Over this period, a total of 1,064,161 data points were recorded.

The M/V KASTOR, constructed in 2020, has a deadweight (DWT) of 81,600 tonnes and a reference speed (V_{ref}) of 14.3 knots [33]. Comprehensive details about the vessel's specifications and a thorough analysis of the ship's electrification system are provided in the previous report of the project (Deliverable 6.1), as outlined by Prousalidis, et al. [34].

2 Fuel Cell/Battery and Waste Heat Recovery Systems

Hybrid system designs focused on ship electrification are especially well-suited for large maritime vessels, where the power demands are lower and more consistent compared to the propulsion. Significant innovations aimed at augmenting or substituting auxiliary engines include batteries [11, 35], WHRS [10, 36] and FCs [19, 37]. Hybrid FC configurations have proven effective in mitigating waterborne emissions and are compatible with a range of alternative fuels [12].

This report evaluates three types of FCs: PAFC, PEMFC, and SOFC, all of which are commercially available and provide suitable power outputs for the case study vessel. Each FC type has its own strengths and limitations, which are analysed and compared in this section. Various power configurations involving FCs, batteries, and WHRS have been identified and analysed from environmental, regulatory, and space-requirement perspectives, including considerations for fuel tank capacity.

2.1 Fuel Cells

A FC is an electrochemical device that converts chemical energy into electrical energy through a reaction between a fuel and an oxidant. It consists of two electrodes: an anode (negative) and a cathode (positive) separated by an electrolyte [38]. H_2 fuel is supplied to the anode, splitting into protons and electrons. Protons pass through the electrolyte to the cathode, while electrons travel through an external circuit, generating an electric current [39, 40]. At the cathode, the protons, electrons, and oxygen (O_2) combine to form water and release heat, providing a continuous and clean power source [41].

FCs, in contrast to batteries, generate power continuously if fuel is fed to the anode and an oxidant (usually air) to the cathode. Unlike conventional power generation methods, they offer numerous advantages, including high efficiency, high power density, compact size, low emissions, minimal noise, and the production of high-quality power. Their modular nature allows them to maintain efficiency even at smaller scales, making them particularly suitable for distributed power generation, which helps reduce transmission and distribution losses [41].

Despite their advantages, FC technologies are still in development and face several challenges that limit their viability compared to established systems. High costs for stationary electricity generation make them economically uncompetitive with fossil fuels. The long-term durability of FCs, particularly high-temperature variants suitable for power generation, remains uncertain. Additionally, H_2 (a primary fuel) remains expensive, and the infrastructure for its production and distribution is underdeveloped. In maritime applications, the safe storage of H_2 in compressed or liquified way is problematic due to its flammability and potential explosiveness [39]. Moreover, FCs have a slower response to rapid load changes unless supplemented by supercapacitors or batteries. These limitations currently prevent FCs from replacing traditional energy technologies [34]. Figure 1 indicates a diagram explaining the working principle of the FC.

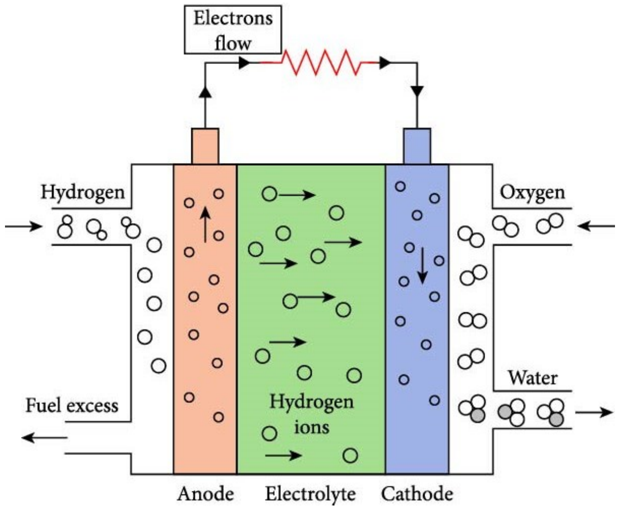

Figure 1: Schematic of the PAFC [41].

In an FC, H_2 is introduced at the anode, where it undergoes an electrochemical reaction. The process is catalysed by platinum, splitting hydrogen gas into protons (H^+) and electrons (e^-). The protons travel through an electrolyte which serves as both a proton conductor and an insulator for electrons, ensuring a controlled flow [42]. Meanwhile, the electrons are directed through an external circuit, creating current flow in the circuit. At the cathode, O_2 reacts with the incoming protons and electrons to form water (H_2O), which is managed efficiently as a by-product. The system also integrates a heat management mechanism to regulate the medium operating temperature, ensuring stable performance. H_2 and O_2 supplies keep the reaction occurring continuously, while water management systems handle the water produced. [43]. Equations (1) to (3) illustrate the reactions occurring at the anode, cathode, as well as the combined system equation within the FC [41].

$$\text{Anode: } H_2 \rightarrow 2H^+ + 2e^- \tag{1}$$

$$\text{Cathode: } O_2 + 4H^+ \rightarrow H_2O \tag{2}$$

$$\text{Overall: } H_2 + \frac{1}{2}O_2 \rightarrow H_2O + \text{Heat} + \text{Electricity} \tag{3}$$

A description of the electrification plant includes a fundamental explanation of their operating principles, relevant modelling equations and the specifications of the commercial FCs considered. Each FC type is examined to highlight its advantages and limitations in a maritime context, with a focus on how it integrates into the ship's power system. The modelling framework employed for simulation is detailed, and key parameters from commercially available FCs are specified to provide a basis for performance evaluation and comparison.

2.1.1 Phosphoric Acid Fuel Cells

PAFCs represent the most prevalent and commercially viable technology among H_2-O_2 FCs, with over 500 power stations constructed and rigorously tested worldwide [43]. They are classified as medium-temperature FC systems, operating within a temperature range of 150 to 220ºC and utilising liquid phosphoric acid (H_3PO_4) as the electrolyte [41]. Further advancements in PAFC technology remain essential to improving power density, extending lifespan and lowering production costs [41]. The limited power density of PAFCs poses a major barrier to broader applications [44]. Recent efforts, both experimental and theoretical, have focused on enhancing power density through material innovations [45], deeper insights into electrochemical mechanisms and transport dynamics

[46]. Performance optimisation at the stack [47] and system levels [48] have also been well studied. The Doosan PureCell 400 has been used as a PAFC option in the analysis of ship electrification. Its specifications are detailed in Table 1.

Table 1: Technical specifications of the PAFC unit used in the analysis [49].

Parameter	Value	Unit
Power	440	KW
Electrical Efficiency	45%	-
LNG Consumption Rate (LNG_{PAFC})	98.4	Nm^3/h
Heat Grade to 121 ºC	162	kW
Heat Grade to 60ºC	292	kW
NO_x	0.009	kg/MWh
SO_x	0	kg/MWh
PM	0	kg/MWh
VOC	0.005	kg/MWh
CO	0.005	kg/MWh
CO_2	454	kg/MWh
Length/Width/Height	8.74/2.54/3.02	m
Length/Width/Height with Cooling Module	4.85/2.39/1.83	m
Weight	28.663	t

An LNG decomposition module has been incorporated into the PAFC system, enabling the breakdown of methane through steam methane reforming to generate the hydrogen gas, needed to fuel the FC. The emissions associated with this process are detailed in Table 1. Moreover, the integration of LNG enhances the practicality of current implementations by diminishing the reliance on hydrogen storage which holds a critical challenge for marine vessels.

The degradation rate of 0.5% per 1000 hours for the PAFC unit has been widely recognised [50] to cause an increase in hydrogen production and a decrease in power generation. The health of the PAFC is assessed using the ratio of actual efficiency (η_{act}) to initial efficiency (η_i). The efficiency curve of the PAFC [51] unit has been used to detect η_i. The unit's lifespan (LT) is defined as either 40,000 operating hours or 10 years, whichever is reached earlier [52]. Equations (4) and (5) outline the calculations for LNG consumption and emissions for the PAFC plant [19].

$$E_{PAFC}\ (t)= \frac{(P_{PAFC} \times C_E \times t \times n_{FC})}{\left(\frac{\eta_{act}}{\eta_i}\right)} \tag{4}$$

$$\text{LNG Consumption } (t)= \frac{P_{FC} \times t \times 0.0007 \times LNG_{PAFC} \times n_{FC}}{\left(\frac{\eta_{act}}{\eta_i}\right)} \tag{5}$$

In the equations above, the power output of a single PAFC is denoted as P_{PAFC} determined in accordance with the requirements of the electrification plant and the available power potential of units. The variable C_E represents the emission coefficient for the FC, as detailed in Table 1, while t is the operation time and n_{FC} signifies the number of active FCs. The LNG consumption is calculated based on the LNG_{PAFC} coefficient presented in Table 1, t of the PAFC, n_{FC} dictated by power demand and a conversion coefficient of 0.007 used to convert Nm^3 into metric tons [19].

2.1.2 Proton Exchange Membrane Fuel Cells

PEMFCs stand out among various FC types due to their simplicity, lightweight design, high efficiency, superior mass power density, absence of waste production, low operating temperature (around 80ºC) and pressure yielding quicker startup, advanced technological maturity and relatively reasonable cost [41, 53, 54]. Their efficiency ranges from 40% to 60% at power outputs exceeding 100 kW and is primarily influenced by size making them a reasonable option for the ship electrification plant [55].

PEMFCs work well under partial load unlike ICEs, and they use water-based, acidic polymer membrane. Recent advancements have led to high-temperature PEMFCs operating at 120–160°C, addressing challenges faced by low-temperature PEMFCs such as water management and the need for ultra-pure H_2 to prevent catalyst poisoning. However, they are more vulnerable to impurities compared to other FC types [55]. In the analysis, the PowerCell Group Marine System 200 PEMFC was employed. Its specifications are detailed as in Table 2.

Table 2: Technical specifications of the PEMFC unit used in the analysis [56]

Parameter	Value	Unit
Power	200	KW
Gross Output DC Voltage	580	V
Gross Output Current	400	A
Electrical Efficiency (Peak)	54%	-
Heat Grade	<320	kW
Fuel Quality	Pure H_2 ISO 14687:2019	-
Length/Width/Height- One Module	0.73/0.9/2.2	m
Weight	1.07	t
Dimensions (width/depth/height)	0.73/0.9/2.2	m

The determination of PEMFC system dimensions and weight require distinct calculations due to the absence of an integrated hydrogen production unit within the cell design. The overall weight and dimensions of PEMFC systems are typically reduced, owing to their high efficiency and the lack of a built-in hydrogen-cracking mechanism. To provide a reliable comparison of the spatial requirements for FC systems, dimensions from an ammonia-cracking system providing high-purity H_2 referenced in the literature [57] have been utilised. The efficiency and specific fuel consumption (SFC) values have been interpolated using the curves in Figure 2.

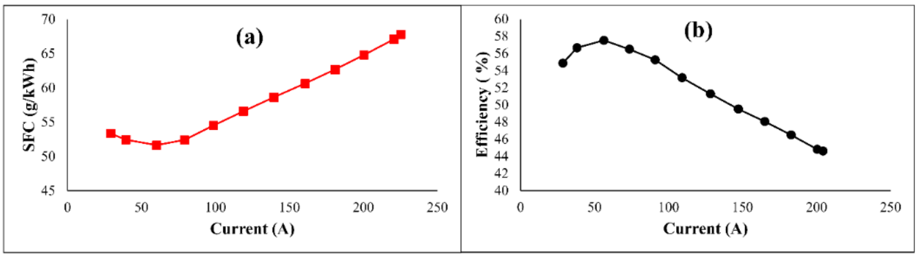

Figure 2: The Current – (a) SFC and current- (b) efficiency curves of PEMFC [56]

The current has been calculated based on the power output of a single PEMFC unit (P_{PEMFC}) which was derived from a comparison between the available power potential of all components and the demand from the ship's grid within the mathematical simulation. The P_{PEMFC} is divided by the ship grid voltage (V_{Grid}) set at 450 V [34] and then multiplied by the inverter's conversion efficiency (η_{inv}) set at 0.984 for the conversion from 800 V Direct Current (DC) to 450 V- Alternative Current (AC) [58]. Equation(6) indicates the calculated PEMFC current (I_{PEMFC}).

$$I_{PEMFC}(A)=\frac{P_{PEMFC}\ (kW)\times \eta_{inv}\times 1000}{V_{Grid}\ (A)} \quad (6)$$

Using the I_{PEMFC} and curves illustrated in Figure 2, the η_i and SFC_{PEMFC} are obtained. Assuming a degradation rate of 0.5% for 1000 h [50] the η_{act} has been updated. The H_2 consumption of the PEMFC has been calculated by employing Equation (7).

$$H_2\ \text{Consumption}\ (t)=\frac{SFC_{PEMFC}\times t\times P_{PEMFC}\times n_{FC}}{\left(\frac{\eta_{act}}{\eta_i}\right)} \quad (7)$$

The LT of PEMFC has been taken at 40,000 hours or 10 years whichever is reached first in the configuration [52]. Operational emissions (OE) from the PEMFC utilising high-purity H_2 are considered negligible and thus have been assumed to be zero.

2.1.3 Solid Oxide Fuel Cells

SOFCs are high-temperature FCs, operating in the range of 600 to 1000 °C, and utilise a ceramic-based solid material as the electrolyte. Alongside PEMFCs, they are among the most efficient types of FCs, with their efficiency further enhanced through the application of a WHRS [12]. Due to their high operational temperatures, SOFCs can accommodate a wide range of fuels, allowing for the integration of an on-board H_2 production unit through the reforming of methane, methanol, ammonia, or even diesel [59]. They also exhibit greater tolerance to fuel impurities compared to PEMFCs, potentially resulting in a longer lifespan. However, a significant limitation of SOFCs is their high operating temperature, which not only increases the start-up time but also demands the use of materials capable of withstanding extreme conditions [60]. A commercial SOFC from FuelCellEnergy has been incorporated into the simulation, with its technical specifications outlined in Table 3.

Table 3: Technical specifications of SOFC unit used in the analysis [61]

Parameter	Value	Unit
Power	250	kW
Output AC Voltage	480	V
Frequency	60	Hz
Electrical Efficiency (Peak)	65%	-
Exhaust Temperature	167	ºC
Exhaust Flow	1,780	kg/h
Fuel Consumption	129	Nm3/h
NOx	0.005	kg/MWh
SOx	0	kg/MWh
PM_{10}	0.00001	kg/MWh
VOC	0	kg/MWh
GHG	0	kg/MWh
Length/Width/Height – One Module	10.66/2.43/3.04	m
Weight	10.2	t

The SOFC unit can operate using both LNG and pure H_2, with the analysis focusing on the pure H_2 scenario. The emission coefficients presented in Table 3 correspond specifically to this scenario. Equation (8) has been employed to compute the H_2 consumption of the SOFC plant.

$$H_2 \text{ Consumption (t)} = \frac{t \times P_{SOFC} \times 3600 \times n_{FC}}{LHV \times \eta_{act} \times 100} \qquad (8)$$

The lower heating value (LHV) of H_2 has been set at 120,000 kJ/kg [62] and the η_{act} is computed by adapting the SOFC performance curves in the literature [63] adjusted to account for a degradation rate of 0.5% over 1,000 hours of operation [50]. The calculation of the SOFC current follows the same methodology applied to the PEMFC, as outlined in Equation 6. LT of the SOFC has been taken at 60,000 hours [64].

2.2 Batteries

Batteries have been employed as a backup for FCs or actively integrated into certain configurations to support the system's performance. Lithium-ion batteries were chosen for this research due to their lack of memory effect, as well as their higher specific energy and voltage compared to other battery types [65]. Table 4 shows the properties of the Panasonic NCR18650GA battery cell used to form the stack.

Table 4: Technical specifications of the battery cell [66]

Parameter	Value	Unit
Capacity	3.45 (typical), 3.35 (minimum)	Ah
Chemistry	Lithium-ion	-
Charging Method	CC-CV	-
Typical Charging Current	1.475	Ah
Typical Charging Time	270	min
Gravimetric Energy Density	224	Wh/kg
Nominal Voltage	3.6	V
Length/Width/Diameter	65/18.5/9	mm
Weight	48	g

The properties presented in Table 4 refer to an individual battery cell. Based on the required battery capacity and a ship grid voltage of 440V, battery packs have been constructed from these individual cells. The charging process employed the Constant Current-Constant Voltage (CC-CV) protocol, which has been also used to guide the battery pack modelling. The voltage drop of the battery during operation has been simulated using the State of Charge (SoC) versus Voltage curves gathered from the manufacturer's datasheet [66]. Figure 3 indicates the SoC and SoH curves.

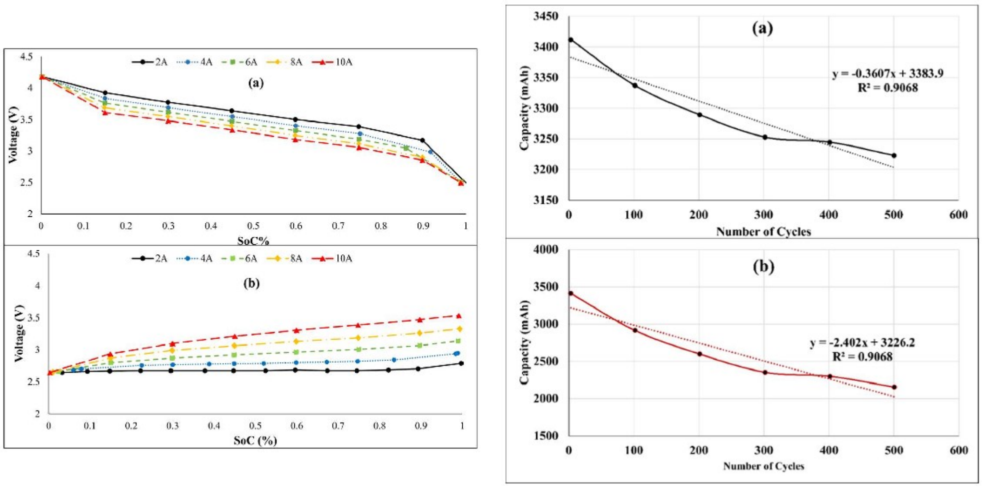

Figure 3: SoC-voltage curves (left) for (a) discharging, (b) charging and SoH curves (right) for (a) C-rate < 1 and (b) C-rate >=1 [66].

The State of Health (SoH) curves were derived from the manufacturer's datasheet, with the slope of each curve varying according to the C-rate (charge/discharge rate). The voltage of the battery stack is determined by fitting the curves shown in Figure 3. The Energy Management Strategy (EMS) determines the operational state of the batteries based on the SoC, which represents the ratio of available battery capacity, while using the fitted curves to calculate the voltage. The time dependent SoC is computed using the conventional Coulomb counting method, as described in Equation (9) [65, 67].

$$\text{SoC (t)= SoC (0)-} \int_0^t \frac{\text{I(t)} \times \eta_C}{C_B \text{ (Ah)}} \tag{9}$$

The EMS maintains the battery's SoC within a range of 20% to 80% to minimise internal resistance, thereby enhancing battery health and extending its lifespan. The coulombic efficiency (η_C) is assumed to be 1, with the charging or discharging current represented as I_B(t) and the battery capacity in ampere-hours denoted as C_B in the formula. A CC-CV charging protocol and CC discharge method are employed to regulate the charging and discharging processes of the batteries.

The capacity reduction due to battery degradation is incorporated into the battery model to update C_B using the SoH curves presented in Figure 4. The battery's capacity loss is calculated iteratively during operation, with adjustments made based on the C-rate. The SoH determined using Equation 10, is defined as the ratio of the C_B after degradation to the initial capacity present (C_i) at the start of operation.

$$\text{SoH (t)= } \frac{C_b \text{ (Ah)}}{C_i \text{ (Ah)}} \tag{10}$$

The battery power (P_{bat}) is derived from voltage calculations based on the State of Charge (SoC) and the I_B. To integrate the DC output of lithium-ion batteries into the ship's AC distribution system, AC/DC converters are employed. Considering an η_{inv} of 0.984, inverter/converter losses are assumed to remain constant during both charging and discharging processes. The AC power from the output of the inverter (P_{inv}), is calculated using Equations (11) and (12) [68].

Discharging: $P_{inv}=\eta_{inv}\times P_{bat}$ (11)

Charging: $P_B=\eta_{inv}\times P_{con}$ (12)

2.3 Waste Heat Recovery System

The WHRS employs an organic Rankine cycle (ORC) to produce electricity from M/E exhaust waste heat. The ORC operates based on the principles of the Rankine cycle, utilising an organic working fluid with a low boiling point to recover heat from low-temperature heat sources. A basic ORC configuration converts waste heat from exhaust gases into useful work, effectively enhancing energy efficiency by utilising otherwise discarded thermal energy [69]. Figure 4 demonstrates the simple-ideal ORC scheme.

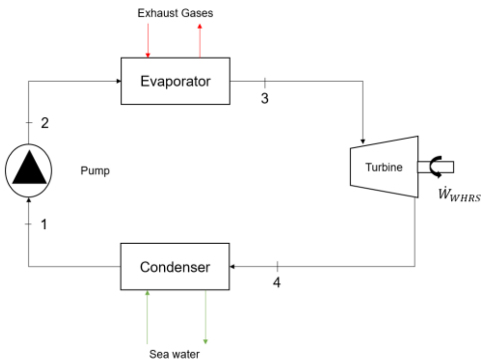

Figure 4. The simple-ideal ORC [70]

ORC consists of four key components: an evaporator, turbine, condenser, and pump. The evaporator recovers waste heat from sources, heating the working fluid and converting it from a compressed liquid to saturated vapor. The high-pressure vapor expands in the turbine, generating electrical energy ($\dot{W}_{WHRS}$) via a connected generator. The condenser then cools the fluid, releasing heat to the environment, while the pump increases the fluid's pressure, completing the cycle [69]. In the analysis, the M/E exhaust gases, as provided in the manufacturer data shown in Table 5, are used as the heat source for the evaporator.

Table 5: Exhaust gas data of M/E

Load	Power	Speed	SFOC	$\dot{m}_{ex}$	$T_{in,\,ex}$
%	kW	r/min	g/kWh	kg/s	°C
25	2483	56.9	175.9	8.7	190
35	3476	63.7	172.8	10	194
50	4965	71.8	167.7	13.9	217
71.6	7110	80.9	166	15.1	205
75	7448	82.1	167.7	19.4	208
100	9930	90.4	172.6	23.7	235

The waste heat sources for the WHRS were the exhaust gases from the M/E after the exhaust gas boiler. The M/E power, RPM, and load were collected from the case study vessel and the exhaust gas amount ($\dot{m}_{ex}$) and evaporator inlet temperatures ($T_{in,\,ex}$) were interpolated from the data. Equation (13) indicates the calculation of $\dot{W}_{WHRS}$.

$$\dot{W}_{WHRS}\ (kW) = \dot{m}_{ex} \times (T_{in,\ ex} - T_{out,\ ex}) \times C_{p,ex} \times \eta_{ORC} \quad (13)$$

The ORC evaporator exhaust outlet temperature ($T_{out,\ ex}$) after the heat transfer in evaporator has been taken to be 100 °C. $C_{p,ex}$ is the amount of thermal energy that, a mass of exhaust emits or absorbs with an alteration in temperature and is taken at 1.089 kJ/kg at stable pressure [71]. The efficiency of ORC (η_{ORC}) has been taken to be 13.2% with a working fluid of R1336mzz(Z) by thermodynamic modelling of the system conducted by Konur, et al. [23]. This η_{ORC} efficiency value has been obtained at an evaporator pressure of 8 bar. The working fluid has a low global warming potential (GWP) and low flammability.

2.4 Internal Combustion Engines

Marine diesel engines (MDEs) are used when the demand exceeds the available FC/Battery and WHRS power. Every hybrid configuration also includes at least one ICE as a backup. Table 6 indicates the properties of the conventional ICE used in ship electrification. Figure 6 illustrates its SFC and power curves with varying engine loads.

Table 6; ICE technical specifications

Parameter	Value	Unit
Model	YANMAR 6EY22LW	-
Bore	220	mm
Stroke	320	mm
Cylinders	6	-
Rated Power	800	kW
Transmitted Power	720	kW
Engine Speed	720	rpm
Fuel	Heavy Fuel Oil (HFO)	
Total Weight	8.416	t
Length/Width/Height	4.478/1.682/2.211	m

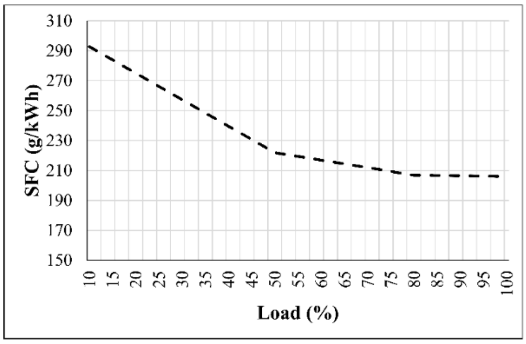

Figure 5: The SFC curve of the marine diesel engine

In terms of fuel requirements, SFC represents the amount of fuel consumed per unit of time to achieve a specific engine output [72]. The curve shown in Figure 6 is used to calculate the fuel consumption of the MDE operating on heavy fuel oil (HFO). The variable load of the diesel generators (D/Gs) is determined through simulation, with the corresponding SFC values applied.

The model calculates the required engine power (P_{ICE}) and the number of active generators (n_{ICE}) for each time interval (t = 1 min). The load and power of each generator were determined in the simulation. Load sharing has been decided using the logic conducted in the study by the Yuksel and Koseoglu [11]. Fuel consumption of the ICEs (F_{ICE}) for each time interval was then calculated using Equation 14.

$$F_{ICE}(t) = \frac{P_{ICE} \times SFC_{ICE} \times t \times n_{ICE}}{1000000} \quad (14)$$

2.5 Modelling Approach

The EMS algorithm and simulation have been designed to manage load-sharing, determine the number of generators or FCs required, and set battery charging/discharging conditions. The simulation, developed in Python, uses the same code infrastructure to evaluate various powertrain options for a hybrid marine power distribution plant. At the start, the user can adjust the configurations and capacities of the FC, battery, and WHRS implementations. The algorithm begins by importing data and necessary libraries, setting initial conditions, and preparing empty lists for data iteration. The simulation operates over grid power data collected for 17,170 hours and sampled at one-minute intervals.

The program first checks if WHRS has been selected as a support option and calculates its power output based on ME power. After determining WHRS involvement, the algorithm decides the number of operating FCs, battery charge/discharge status, and engine load. FC and battery capacities are adjusted according to the hybrid scenario and FC type, while WHRS power availability influences the determination of parameters. Battery performance is managed by the EMS based on charge/discharge status, keeping the SoC between 20% and 80% to maximise battery lifespan.

In scenarios involving FCs, the FCs handle battery charging, using previously established SoC-voltage curves to account for voltage drop and available battery power. Simultaneously, the SoH is calculated. Next, the required engine power is determined to identify the number of operational D/Gs, and HFO consumption is estimated using the curve in Figure 5.

The calculated parameters during each loop are stored in pre-initialised lists, which are then exported to spreadsheets for analysis at the end of each iteration, before being cleared for the next round. After determining the total fuel consumption for each hybrid scenario, additional assessments are performed, including fuel tank capacity design, well-to-tank/tank-to-wake (upstream/operational) emissions calculation, and EEXI evaluation.

2.6 Emission Calculation

The operational emissions from ICEs have been determined by multiplying the operational emission coefficients for HFO provided by the F_{ICE}. Similarly, the upstream emissions associated with the fuels used in ICEs and FCs were calculated using the upstream emission coefficients. This approach ensures consistency in evaluating both operational and upstream emissions based on the coefficients and consumption values specified in the dataset. Table 7 indicates the operational and upstream emission coefficient values.

Table 7: Operational and upstream emission coefficients.

Operational emission coefficients of conventional fuels (g emission/ g fuel) [73]							
Fuel	**CO_2**	**N_2O**	**CH_4**	**NO_x**	**SO_x**	**PM**	**VOC**
HFO	3.114	0.00015	0.00006	0.903	0.025	0.00278	0.00308

Upstream emission coefficients of fuels used in the configurations (g UE/ g OE) [14, 74, 75]						
Fuel	**CO_2**	**N_2O**	**CH_4**	**NO_x**	**PM**	**SO_x**
HFO	0.147	0.004	0.879	0.010	0.022	0.102
LNG	0.131	0.004	0.879	0.007	0	***0.158**
H_2	***110.902**	0.000	0.000	***0.191**	***1.145**	***0.141**

*Unit is g/kWh in these coefficients.

Using the operational CO_2, the EEXI calculations have been ensured for the case study bulk carrier using the framework presented in Spiteri, et al. [33], Prousalidis, et al. [34].

The equivalent CO_2 ($CO_{2\text{-eq}}$) indicating 100 years of GWP has been calculated for considering both operational and upstream GHGs by using Equation15 [76].

$$CO_{2\text{-eq}} = CO_2 + 265 \times N_2O + 28 \times CH_4 \quad (15)$$

The increased GWP potential of N_2O and CH_4 has been indicated by employing the coefficients presented in Equation 15 provided in IMO Life Cycle Assessment guidelines [76].

2.7 Integration of Hybrid System

The conventional marine power distribution system comprises of three D/Gs with a 720-kW power output capacity working in parallel. The vessel's electricity demand determines the number of generators in operation [11]. The case study has evaluated the implementation of FCs (i.e. SOFC, PEMFC, and PAFC), batteries and WHRS combined and individually. Their suitability, sizing, and application scenarios have been analysed with respect to environmental impact and space requirements in maritime contexts. The operation of the D/G and its power capacity distribution has been assessed across different scenarios combining FCs, batteries and WHRS, considering both full electrical demand and partial load-sharing between the D/G and alternative systems. Table 8 presents the system configurations for load-sharing scenarios involving MDEs and FCs, as well as the associated equipment weights and volumes. Figure 6 demonstrates a schematic of the simplified system for the assessed hybrid electrification systems.

Table 8: Hybrid configurations.

Equipment	Numbe r of A/Es	Numbe r of FCs	FC Power (kW)	Battery Capaci ty (kWh)	WHRS Power (kW) @ 75% Load	Weig ht (t)	Equipm ent Volume (m^3)
Base: MDE	3	0	0	0	0	25.25	49.96
Case 1: MDE/SOFC/Batteries/WHRS	2	1	250	273.00	197	28.62	43.87
Case2: MDE/PEMFC/Batteries/WHRS	2	2	400	123.00	197	19.69	35.61
Case 3: MDE/PAFC/Batteries/WHRS	2	1	440	83.00	197	45.98	62.08
Case 4: MDE/WHRS/Batteries	3	0	0	600	197	11.90	17.45

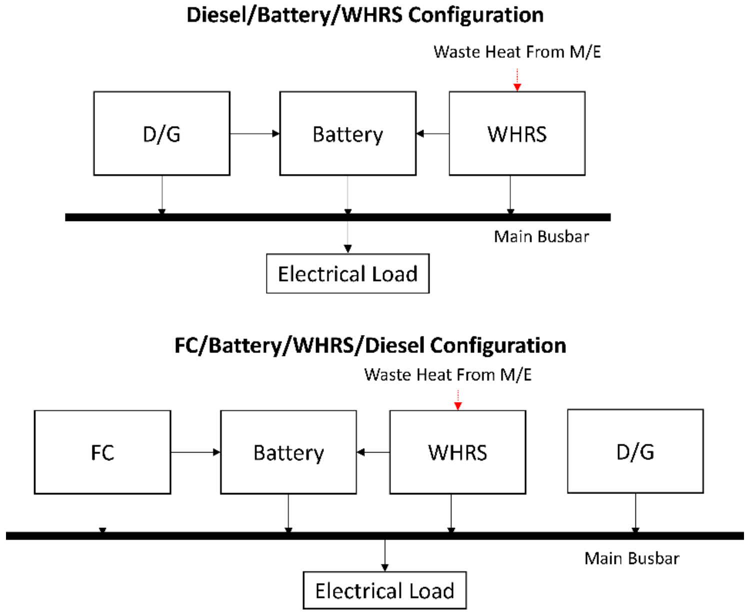

Figure 6: The investigated hybrid designs for marine power distribution unit.

The layout schemes for the FC-integrated hybrid scenarios have been created using CAD software by assuming a 1.8m distance between each equipment to determine the total required space and volume. Due to the significantly high dimension requirements of the FC system, only their layouts have been presented. The base scenario, battery/WHRS, and sole WHRS scenarios have been calculated directly based on the dimensions provided in the technical data sheets of the respective equipment. Figure 7 illustrates the layout plans for scenarios incorporating FCs.

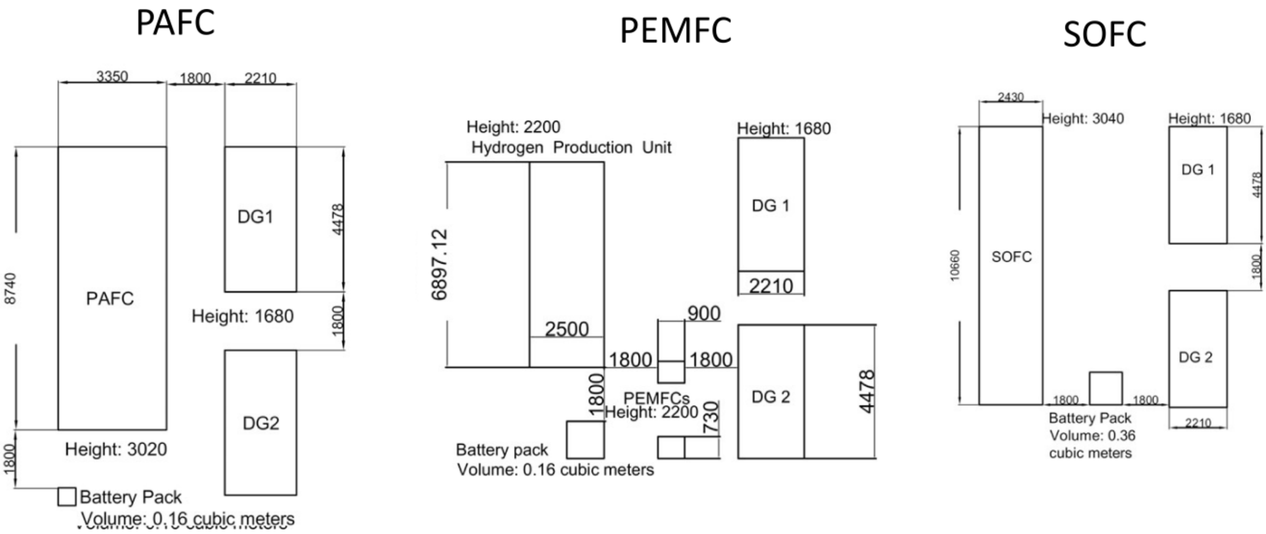

Figure 7: FC layout schemes.

For the PEMFC, the dimensions of an example H_2 production unit have been used for calculations. PAFC and SOFC applications utilise a single FC due to space constraints. Conversely, two FCs are employed in PEMFC configurations.

3 Shaft Generator/motor (PTO/PTI)

The PTO/PTI, also called the shaft generator/motor, technologies are one of the most promising solutions for reducing fuel consumptions. PTO/PTI is a key feature of the hybrid propulsion paradigm [78-80].

The main advantages of these retrofitting technologies are more efficient electric power generation due to higher efficiency and lower SFC of the M/Es compared to the auxiliary ones, and the associated reduced maintenance costs.

The main motivations leading to the adoption of PTO/PTI technology are the following:

- It reduces the need to burn extra fuel to power electrical systems through separate diesel gensets.
- Fuel savings are significant, especially when coupled with improved operational flexibility.
- The system can drastically decrease the operating hours of auxiliary generators and their need for maintenance.
- It helps the M/Es s to run at a more efficient operating point with lower fuel consumption.

The main benefits are listed as follows:

- Small space requirement
- Low installation cost
- Low noise levels
- High reliability

On the contrary, the main drawbacks are:

- No electric power generation while in port
- Increased load on the M/E of the ship

The mechanical connection of an electrical machine on the shaft of the M/E, typically by dual-in/single-out reduction gearbox, can be exploited to fulfil the tasks described hereinafter.

In PTO generator, commonly known also as a shaft generator, part of the mechanical power from the propulsion engines is transformed into electrical power and transferred into the shipboard power grid by a gearbox and an electric generator. Such a configuration has proven to be, the most efficient way to produce the electrical power, instead of running an additional engine to produce it (auxiliary generators). PTO systems are coupled to the main propulsion engine and generate electricity supplied either directly to the main ship grid or to specific loads onboard. For frequency variations and voltage matching, a complete drive chain is required for utilising the energy.

The main advantages of these systems lie in more efficient electric power generation due to the higher efficiency of the M/Es compared to the auxiliary ones, as well as the associated reduced maintenance costs. Furthermore, via this operation, PTOs can improve the efficiency of the main propulsion engine, as they can shift its operating point closer to its minimum consumption region.

3.1 PTO/Gear Constant Ratio (PTO-GCR)

The configuration shown in Figure 8 is called PTO/gear constant ratio (PTO-GCR) [81]. In such a configuration the electric frequency of the generator is proportional to the speed of the propulsion engine, implying that constant frequency production is only possible when the ship navigates at sea. If constant frequency is to be generated, either a controllable pitch propeller should be installed, or an induction generator used. A different way to obtain constant frequency is the so-called PTO/constant frequency mechanical (PTO/CFM). In such a configuration, a speed controlled planetary gearbox is integrated in the system, permitting constant speed of the generator to be achieved within a certain speed range of the propeller. This enables parallel operation with the ship's D/Gs.

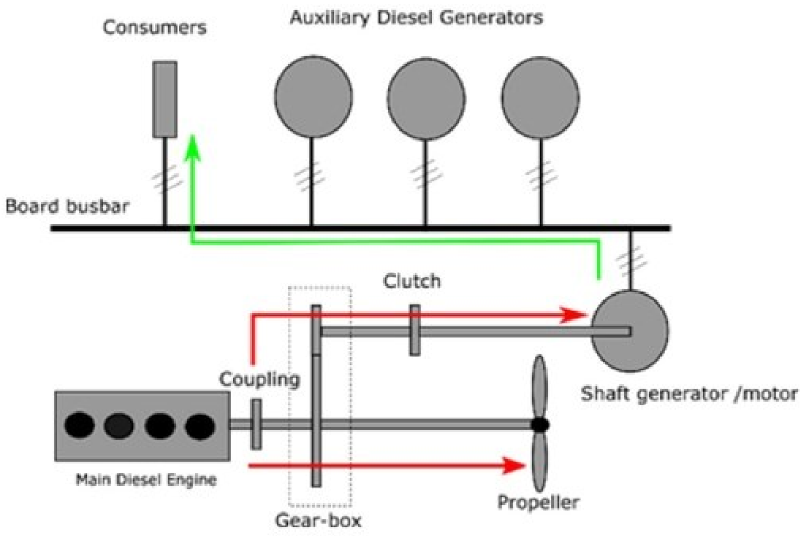

Figure 8: Typical PTO schemes: PTO-CGR system with power flows (red: mechanical, green: electrical)

3.2 PTO/Constant Frequency Electrical (PTO-CFE)

An improved configuration is called PTO/constant frequency electrical (PTO-CFE) [81], as shown in Figure 9 Such a configuration is based on a step-up gear, generator and electrical control equipment decoupling the shaft generator from the on-board grid frequency. Finally, the gearbox can be avoided by using a slow-running generator, directly mounted on the front end of the M/E shaft as shown in Figure 10.

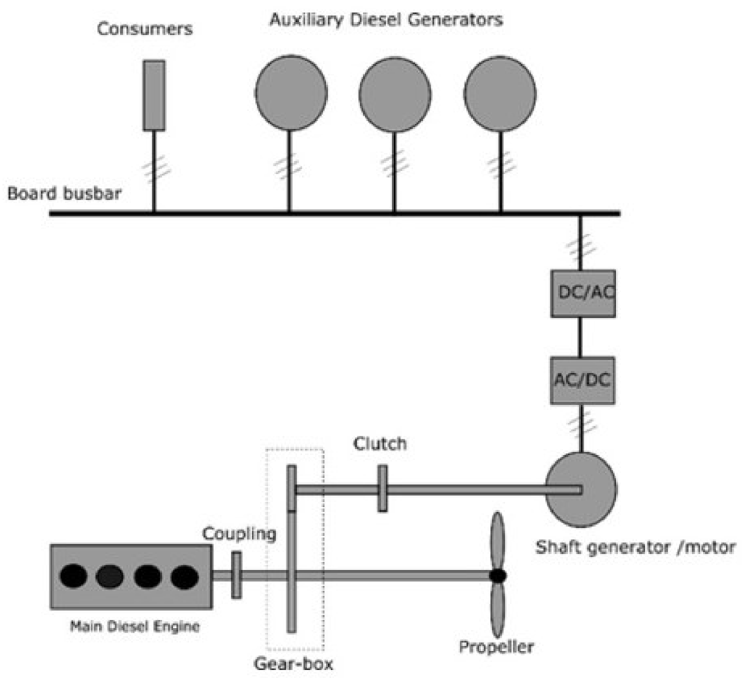

Figure 9: Typical PTO schemes; PTO-CFE system with gearbox

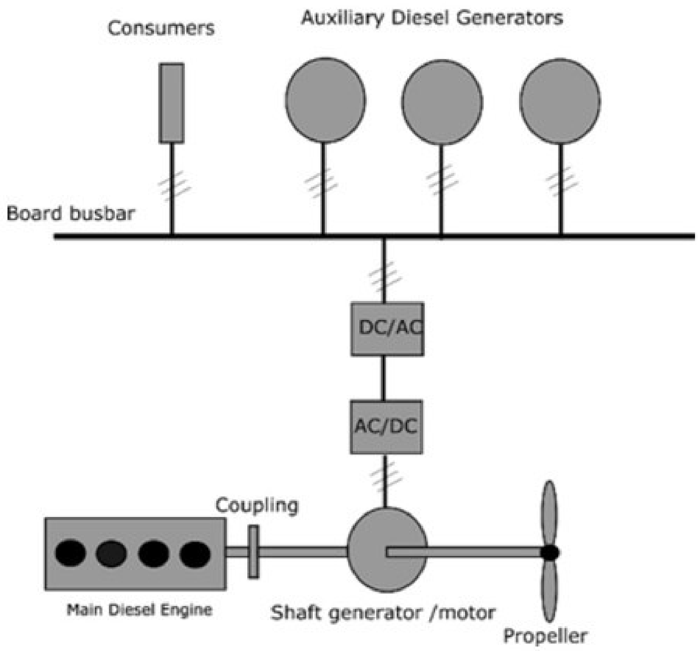

Figure 10: Typical PTO schemes; PTO-CFE system with low-speed generator

In PTI, i.e., propulsion electrical motor mode of operation, the shaft generator is operating as a synchronous motor (electrical power being supplied by the vessels auxiliary diesel generator sets).

It can either provide a boost in power, working alongside the M/E to increase vessel speed, or allows the main engine to reduce power, thereby lowering fuel consumption and wear on the M/E. In this PTI mode of operation, the shaft generator does not require a self-starting capability, because under normal circumstances, it will already be spinning as an alternator before switching over to motor mode. It can be exploited for electrical propulsion for several options of utilisation, as shown in

Figure 11.

Electrical mode is typically adopted during periods of low power demand. for Examples of these periods include sailing out from harbour or running the vessel in emission-free sea areas where specific restrictions are valid (if energy storage is used as a source of energy). Hybrid mode is typically adopted either to improve propulsion engine performance or to boost the speed/ or thrust of the propulsion drive train to the maximum amount. This mode reveals a very interesting option, in terms of vessel design, whereby the operation profile contains short time intervals of full power, as harbour tugs often do, or in cases involving a small propulsion engine.

A further operation mode, typically adopted in the case of an absence of the M/E to increase the redundancy of the propulsion system, is the so-called power-take-home (PTH); which is schematised in Figure 12. The shaft generator is operating as a synchronous motor. In this case, it provides for 100% of the ship's propulsion power. Unlike PTI mode, in PTH the shaft generator requires a self-starting capability to operate as a motor from zero speed. There are different methods that can be employed for starting the shaft generator when it is used in the PTH mode as a motor, the most common of which are: the pony motor start, the autotransformer start, the excitation start, and the variable frequency drive (VFD) start. In the last case the shaft generator is controlled through a VFD unit, which gradually rotates the generator shaft, ensuring that the correct amount of shaft torque is delivered while limiting the current, until the synchronous speed is achieved.

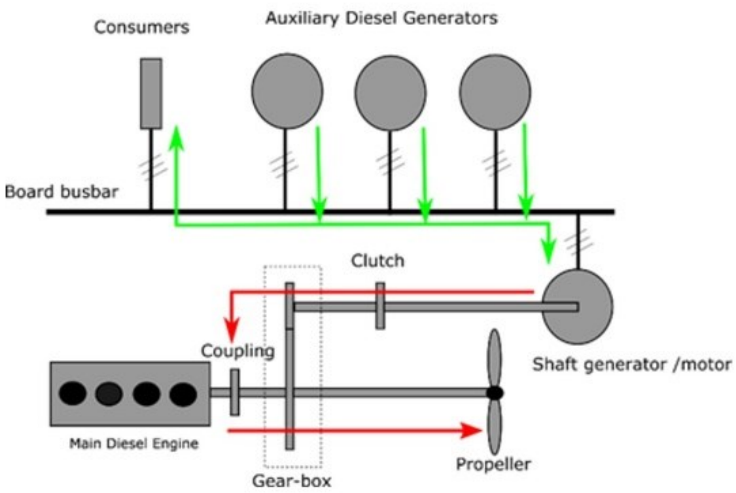

Figure 11: PTI system with power flows (red: mechanical, green: electrical)

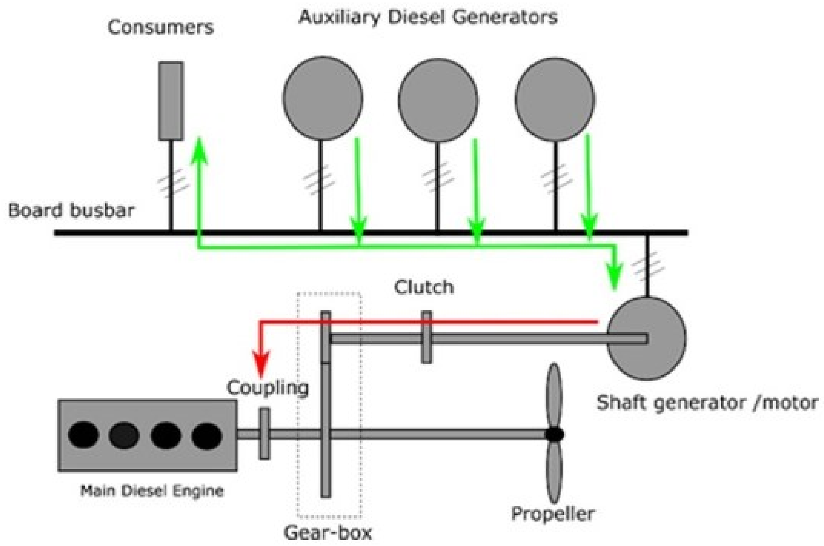

Figure 12: PTH system with power flows (red: mechanical, green: electrical)

3.3 Ship Types Suitable for PTO/PTI Integration

The PTO/PTI technique is commonly used as a retrofitting measure on various types of ships, particularly those aiming to optimise energy efficiency and operational flexibility. Below are the main categories:

Cruise ships are among the primary users of PTO/PTI technologies because of the need to manage a high electric energy demand for passenger comfort (air conditioning, lighting, and services). This system allows on the one hand, the generation of electrical power through PTO by utilising excess energy produced by the M/Es. On the other hand, increased power for propulsion is available when needed through PTI, using electric motors as support.

Even merchant ships exploit PTO/PTI technologies. Among merchant ships, there are:

- Container ships: They benefit from the PTO/PTI system to efficiently manage energy demands, particularly the energy required by onboard cranes and container cooling systems.
- Bulk carriers and tankers: These use PTO/PTI to optimise fuel consumption, as they at reduced speeds on long routes.

Offshore support vessels, such as mobile platforms and pipe-laying ships, frequently use PTO/PTI. This allows them to power specific onboard equipment without relying exclusively on D/Gs and enhances manoeuvrability and precision during anchoring or installation operations.

Military ships, such as frigates or destroyers, integrate PTO/PTI into hybrid propulsion systems to reduce fuel consumption during low-speed operations as well as to provide sufficient power for weapons and radar systems without needing to start dedicated generators.

Ferries and Ro-Pax Ships combine the transport of passengers and vehicles. The PTO/PTI system, in this specific case, is used to power onboard systems, especially when docked at the port and offers greater flexibility in power management during voyages.

Oceanographic and scientific research ships often require flexible energy configurations, that are made possible by PTO/PTI. They can adapt energy production to scientific equipment without compromising propulsion performance.

Finally, electric ships or hybrid electric propulsion ships greatly benefit from PTO/PTI to maximise efficiency between diesel engines, gas turbines, and electric motor as well as to optimise range and fuel savings.

The specific application of PTO/PTI technologies on bulk carrier ships, as the Kastor ship, which is investigated in the RETROFIT55 project, offers interesting opportunities to improve energy efficiency, but there are also some limitations to consider. The main advantages for integrating PTO/PTI in bulk carrier ships are the improved energy efficiency, the operational flexibility, and the environmental sustainability.

As for the improved energy efficiency, such technology permits the optimisation of the available energy, given that bulk carriers often operate on long routes at constant speeds. The PTO system allows excess energy from the M/Es to be converted into electricity to power onboard systems, reducing reliance on auxiliary generators. At the same time, a reduced fuel consumption can be achieved from the PTI operation, because electric motors can assist propulsion during manoeuvres or loading/unloading phases, optimising fuel use.

During manoeuvres requiring rapid power changes, the system may not respond as effectively as a traditional diesel-electric setup for operation at reduced speeds without fully engaging the M/E, which is useful when entering ports or navigating ecologically sensitive areas. Moreover, it permits an increased adaptability to energy loads, given that excess energy can be used to power auxiliary systems, such as machinery for cargo handling (cranes or conveyors).

As for the environmental sustainability, the adoption of PTO/PTI permits the reduction of emission in terms of optimized use of the M/Es and reduced reliance on generators that lower CO_2 emissions and other pollutants. Moreover, the system helps bulk carriers meet strict international regulations (such as MARPOL and IMO 2020) on emissions.

The main drawbacks arising from the adoption of PTO/PTI on bulk carrier ships are the system complexity, the dependence on operating conditions, the added weight and space requirements. As a matter of fact, implementing a PTO/PTI system requires significant upfront investment and specialized maintenance, and the integration of the system necessitates a highly skilled crew to manage and maintain the equipment. In addition, the effectiveness of the PTO depends on the load and operational regime of the M/E. At low loads, the energy available for the PTO might be insufficient for power auxiliary systems. In addition, during manoeuvres requiring rapid power changes, the system may not respond as effectively as a traditional diesel-electric setup. As for the space requirements, adding a PTO/PTI system, along with its components (such as alternators, converters, and cabling), can increase the ship's overall weight and reduce the space available for cargo. The added weight might lead to a slight increase in fuel consumption during certain phases of the voyage.

The following examples of existing bulk carriers utilising PTO/PTI systems demonstrate how the technology enhances energy efficiency and environmental performance:

- *Hagland Hybrid Bulk Carriers*: These 5,000 DWT self-discharging hybrid bulk carriers (see Figure 13) incorporate battery systems alongside PTO/PTI technology. During long-distance transit, the system enables peak shaving through electric motors, reducing fuel consumption. It also allows for zero-emission operations in ports and environmentally sensitive areas like fjords. The vessels comply with IMO Tier III regulations, significantly lowering CO_2 and NO_x emissions.

- *ECO-Ship 2020 Concept*: Developed by Oshima Shipbuilding and DNV, this innovative open-hatch bulk carrier (Figure 14) integrates a flexible propulsion and power generation system, including a PTO/PTI. It features LNG-fuelled engines, waste-heat recovery to power the PTI and energy-efficient designs. These features aim to achieve fuel savings of approximately 5% and CO_2 emission reductions of up to 50% compared to traditional bulk carriers.

Figure 13: Hagland Hybrid Bulk Carriers

Figure 14: ECO-Ship 2020 Concept

3.4. Integrating the PTO/PTI Technology in the Kastor ship

With specific regard to the bulk carrier, Kastor, the vessel that is being investigated in the RETROFIT55 project, the M/E propelling the ship is the MAN B&W S60ME-C8.5-TII [82]. Figure 15 shows the engine cross section, with reference to the turbochargers mounted on the exhaust side.

The service range is limited by four lines: 4, 5, 7 and 3 (9), shown in Figure 16. The propeller curves, overload limits and lines 1, 2 and 6, in the load diagram are also described below.

M: Specified MCR (Maximum Continuous Rating) point

- Line 1: Propeller curve through point M (i = 3) - (engine layout curve)
- Line 2: Propeller curve, fouled hull and heavy weather – heavy running (i = 3)
- Line 3: Speed limit
- Line 4: Torque/speed limit (i = 2)
- Line 5: Mean effective pressure limit (i = 1)
- Line 6: Propeller curve, clean hull and calm weather – light running (i = 3), for propeller layout. The hatched area indicates the full recommended range for LRM (4.0-10.0%)
- Line 7: Power limit for continuous running (i = 0)
- Line 8: Overload limit
- Line 9: Speed limit at sea trial

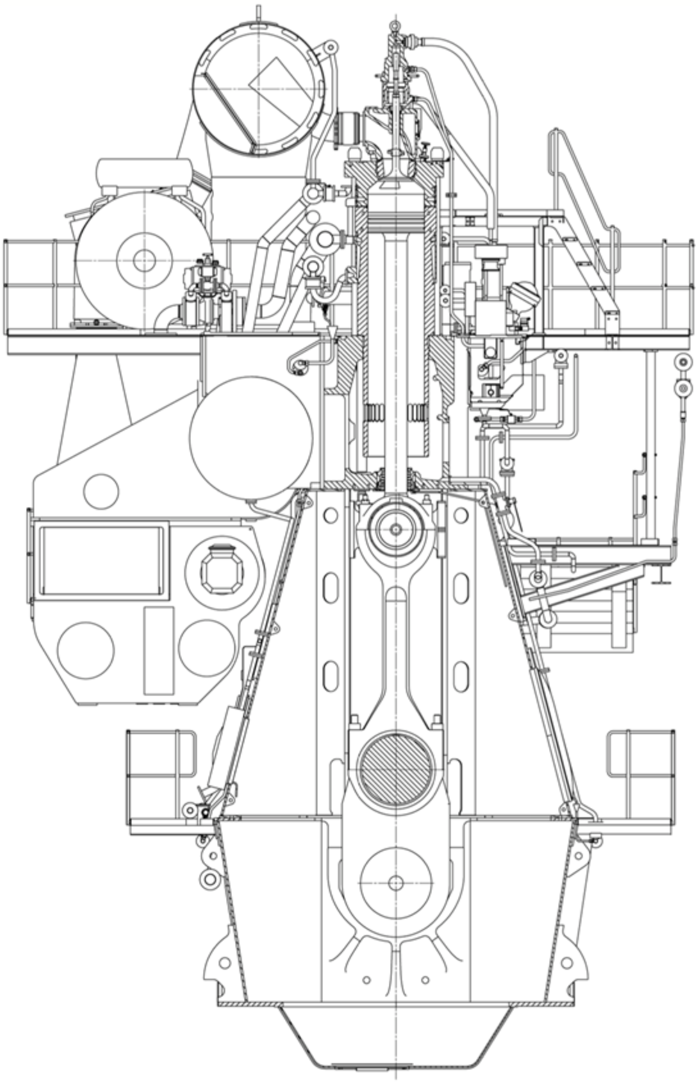

Figure 15: Engine cross section, turbocharger(s) mounted on the exhaust side.

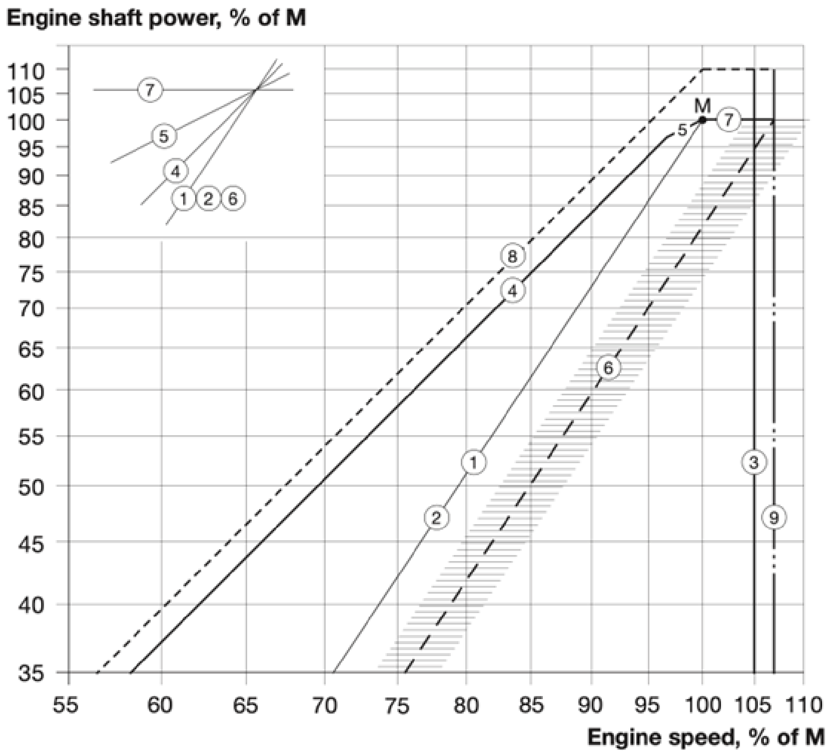

Figure 16: Engine shaft power vs engine speed (from MAN [82]])

The recommendation provided by MAN [82], useful for the integration of PTO/PTI technologies, are the following. The area between lines 1, 3 and 7 is available for continuous operation without limitation. The area between lines 1, 4 and 5 is available for operation in shallow waters, in heavy weather and during acceleration, i.e. for non-steady operation without any strict time limitation. The area between lines 4, 5, 7 and 8 is available for overload operation for 1 out of every 12 hours.

After some time in operation, the ship's hull and propeller will be fouled, resulting in heavier running of the propeller, i.e. the propeller curve will move to the left from line 6 towards line 2, and extra power is required for propulsion to keep the ship's speed.

In calm weather conditions, the extent of heavy running of the propeller will indicate the need for cleaning the hull and polishing the propeller.

As for the electricity production on board, the MAN B&W S60ME-C8.5-TII engine is already designed for integrating the PTO/PTI technology, see section 4.01 in [82],. Several standardised PTO systems are available, see Figure 17 from [82],:

- PTO/RCF (Power Take Off/Resonant Constant Frequency): Generator giving constant frequency, based on mechanical/hydraulic speed control.
- PTO/CFE (Power Take Off/Constant Frequency Electrical): Generator giving constant frequency, based on electrical frequency control.
- PTO/GCR (Power Take Off/Gear Constant Ratio): Generator coupled to a constant ratio step/up gear, used only for engines running at constant speed.

The DMG/CFE (Direct Mounted Generator/Constant Frequency Electrical) and the SMG/CFE (Shaft Mounted Generator/Constant Frequency Electrical) are special designs within the PTO/CFE group whereby the generator is coupled directly to the M/E crankshaft or the intermediate propeller shaft, respectively, without a gear. The electrical output of the generator is controlled by power converters.

Within each PTO system, several designs are available, depending on the positioning of the gear:

- BW I: Gear with a vertical generator mounted onto the fore end of the diesel engine, without any connections to the ship structure.
- BW II: A free-standing gear mounted on the tank top and connected to the fore end of the diesel engine, with a vertical or horizontal generator.
- BW IV: A free-standing step-up gear connected to the intermediate propeller shaft, with a horizontal generator.

Based on the desiderata of the case study ship, the PTO/CFE configuration with the DMG solution has been chosen, since it permits the highest controllability and flexibility in the use of the shaft generator as well as the highest capability to minimise the fuel consumptions and polluting emissions. As for the positioning of the gears, this issue has not still been tackled. Figure 18 shows the engine preparation for PTO, as reported in the manual of the MAN B&W S60ME-C8.5-TII engine.

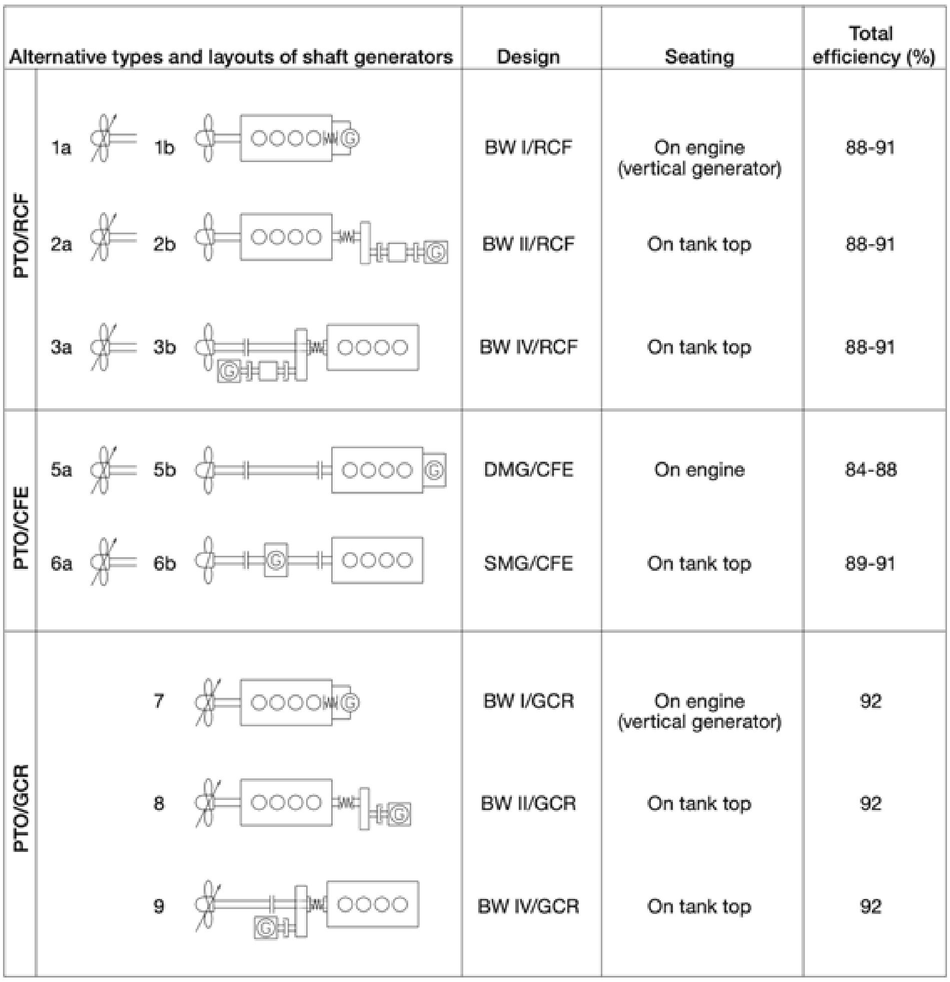

	Alternative types and layouts of shaft generators	Design	Seating	Total efficiency (%)
PTO/RCF	1a 1b	BW I/RCF	On engine (vertical generator)	88-91
	2a 2b	BW II/RCF	On tank top	88-91
	3a 3b	BW IV/RCF	On tank top	88-91
PTO/CFE	5a 5b	DMG/CFE	On engine	84-88
	6a 6b	SMG/CFE	On tank top	89-91
PTO/GCR	7	BW I/GCR	On engine (vertical generator)	92
	8	BW II/GCR	On tank top	92
	9	BW IV/GCR	On tank top	92

Figure 17: Types of PTO (from [82])

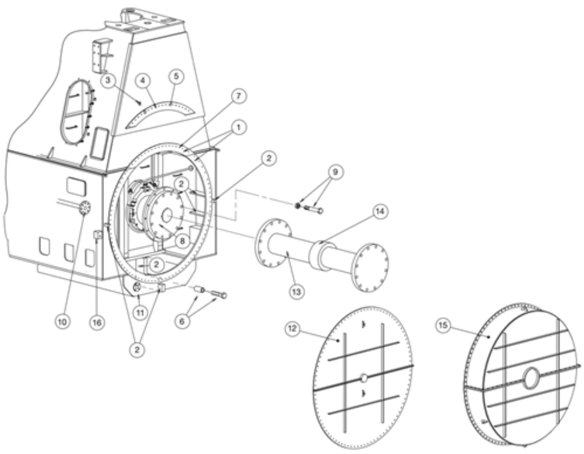

Figure 18: Engine preparation for PTO (taken from [82])

4 Exploitation of Integrated Photovoltaic solutions

This section describes the results obtained as part of the analysis aimed at evaluating the potential for integrating PV generation systems on the cargo ship chosen as a case study, namely the bulk carrier M/V KASTOR, operated by LASKARIDIS SHIPPING CO., LTD., whose main features are described earlier in this deliverable. Following an introduction which outlines the most relevant features of PV generation and highlights the pros and cons of its use in the maritime environment, the following points are addressed:

- The available surfaces on the ship under study are evaluated and a selection of PV panels suitable for such application is proposed.
- The maximum installed PV power on the case study ship is determined using an automatic PV panel configurator, specifically designed to optimise the installed power based on the given geometric and electrical characteristics of the PV panels.
- The main balance of plant's (BOP) components is identified by pointing out their relevant properties.
- Challenges in evaluating actual PV power production and possible outcomes from the synergistic use of PV and other electrical efficiency-oriented technologies are addressed.

4.1 Introduction to the use of PV on ships

The primary role of PV in the global transition towards a low carbon energy mix has been consolidated over the past two decades. PV power generation reached 945.7 GW at the end of 2021 and currently contributes to reducing annual global emissions by about 3% [78]. The year 2022 was a milestone year for PV, with cumulative installed global capacity exceeding 1 TW. Indeed, PV represented 56% of newly installed global electricity generating capacity for 2022, the second year in a row that this metric exceeded 50% [83].

The growing competitiveness of PV systems, along with the potential to integrate solar generators with storage systems, IoT devices, advanced monitoring, communication, and EMS, is facilitating the shift towards smart grid electricity systems. Additionally, the rising electrification of transportation and the demand for green hydrogen production are accelerating the incorporation of PV generation into vehicles, infrastructure, buildings, and various other sectors that consume energy [84-86].

Despite such an extensive use of PV in terrestrial applications (e.g., at utility scale), the shipboard integration of PV generation systems is limited so far. Indeed, the requirement of a large surface area on board for installing PV panels, has made the use of solar-assisted power generation on ships quite uncommon [87].

Currently, the need for implementing the mandatory measures encouraging the adoption of energy-saving technologies in ships, according to IMO GHG strategy to 2050 [88], is pushing players of the shipping industry toward considering the integration of on-board PV systems as a viable solution contributing to fuel consumption and pollutant emission reduction [28].

The PV technology is considered a suitable solution for ship retrofitting. According to [89], PV systems can operate as an ideal additional source of auxiliary power, since they feature all the following main properties:

- electrical power production not involving transfer of gas or liquid fuel,

- electrical power production not implying gas and noise emission,
- practical absence of mechanical moving parts,
- simplicity, ease of installation and fast replacement in case of aging or degradation,
- possible installation on surfaces with no practical use and/or on preexisting structures (e.g., roofs, walls, hold covers, etc.),
- long lifetime and low maintenance cost.

The main drawback of PV solar power is the high capital cost of these plants that have not yet benefited from large scale economies in the maritime sector. Cargo vessels present at least the following two advantages that make them suitable for the implementation of PV modules:

- they have little equipment installed on top of their deck,
- they have a relatively large surface area that is only used to store goods, i.e., the hold, upon which PV modules can be appropriately integrated [84].

Cruise ships are also under consideration for photovoltaic application, notwithstanding the limited availability of space on the hull. Given the large number of cabins and balconies, the possibility of installing conventional PV panels on such structures was evaluated in Schwager, et al. [90], where the effects of partial shading were considered, and different string configurations were evaluated.

Some studies on shipboard PV integration have also been conducted with a focus on naval vessels [91]. These investigations revealed a dual benefit—both economic and environmental—despite the drawback of an increased infrared signature, which makes the ship more detectable. Additionally, PV integration is gaining attention in the Ro-Ro marine vessel sector, where a recently developed design/layout approach showed a 7.38% reduction in fuel consumption for the case study vessel [89].

The growing interest in implementing PV generation in the marine environment is reflected in the development of numerous scientific and industrial projects focused on demonstrating innovative solutions for the rapid and effective decarbonisation of shipping. Ongoing industrial and scientific research is exploring shipboard PV generation, including its installation in hybrid configurations.

A survey of industrial solar ship projects developed in the last two decades is presented in Paulson and Chacko [28].

A further example worth mentioning is the maritime industry's first installation and commissioning of a hybrid power system including a PV generator on board a bulk carrier vessel, described in [30]; particularly, the use of Flettner rotors in combination with PV panels on bulk carriers is analysed to determine the contribution of renewables to the propulsion and to assess their impact on the attained EEDI through calculation using IMO's guidelines. In addition, a joint venture comprising of a ship design company, a shipping company and wind propulsion specialists is developing a project to retrofit a 203,000 DWT Newcastlemax bulk carrier having a CII rating of Category D so as to make it compliant with EEXI and CII and raise it to category C [29]. This project involves the on-board installation of a PV/battery generation system to reduce the hours in service for the auxiliary engines, while taking advantage of the free area on deck. The CO_2 emission reduction is estimated to be around 6%, which is equivalent to about 3.300 tons of CO_2 reduction per year for the considered case study.

Figure 19 shows an example of shipboard PV panels installed on a car carrier ship.

Figure 19: PV panel installation example on a car carrier ship [92].

The EU-funded Engimmonia, project, for example, is promoting the transfer of clean energy technologies like renewables, that have been successfully demonstrated in terrestrial applications, to the maritime sector. In particular, the installation of PV composite surfaces easily installable on vessel structural parts is under consideration for three different kinds of vessels (i.e., an oil tanker, a ferry, and a container ship) [32].

The application of solar PV technology on board vessels is still in its early stages, and many countries are actively working on its development and enhancement. There is still much progress to be made in this area. Furthermore, due to the variations in the structure, purpose, and operational routes of different ship types, it is not feasible to arbitrarily select a ship as a simple platform for solar panel installation [93].

The selection of the target ship type should be based on a thorough evaluation and analysis, considering factors such as capital cost, safety regulations, and optimal use of space. Additionally, the efficiency and reliability of PV generators must be carefully considered, including potential issues such as corrosion and the impact of vibrations on solar panels in marine environments.

In summary, shipboard PV systems present unique challenges due to the distinct characteristics that differentiate them from land-based PV systems. However, they offer promising potential as a valuable option for supplementing auxiliary power generated by diesel-electric systems, thereby improving energy efficiency, and promoting environmental sustainability in the maritime sector.

4.2 Application to the case study ship (M/V Kastor)

This section examines the integration of a PV system on the M/V Kastor ship as an electrical retrofitting solution, specifically as an additional auxiliary power source. The focus is on installing a PV array using highly efficient panels, previously tested in maritime applications. The study considers best practices for PV panel installation on ships and explores effective strategies to maximise installed power, considering the electrical and geometric characteristics of both the PV panels and the ship itself.

4.2.1 Assessment of available spaces for panel installation

The first step in evaluating the potential power production of an integrated PV system is to assess the available surfaces on board the ship that can be dedicated to PV panel installation. To obtain this crucial information we used the technical/constructive data of the ship provided by the ship owner

(Laskaridis Shipping Co., Ltd.) in particular, we referred to the general arrangement plans of the ship, whose longitudinal section and top view are shown in Figure 20.

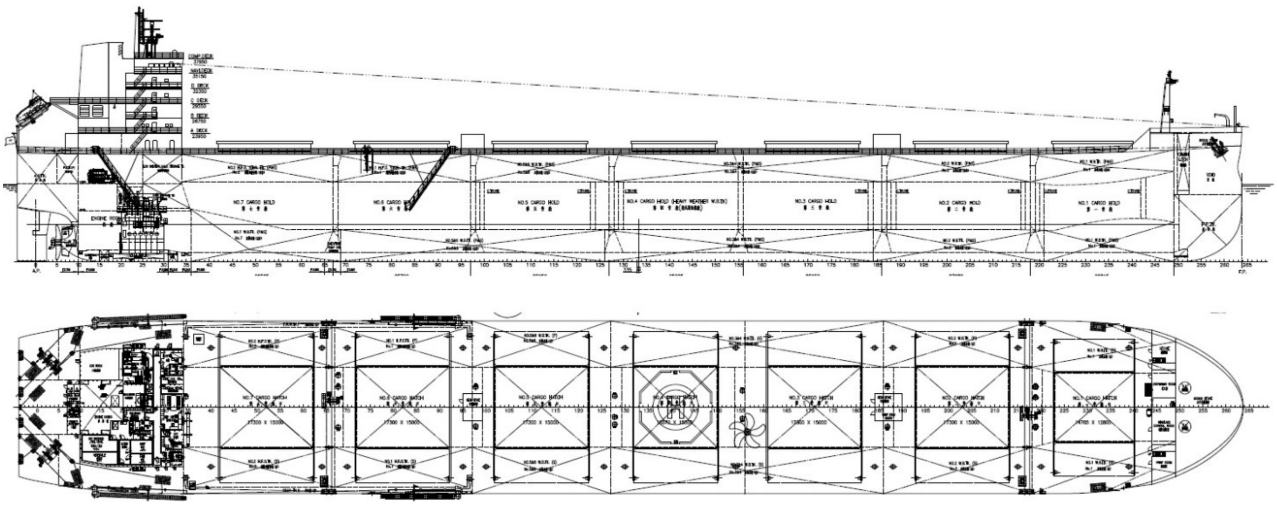

Figure 20: Longitudinal section and top view of M/V KASTOR ship.

It was observed that most of the available surfaces are located on deck A on which there are seven hatch covers and several walkways. The total area of deck A is about 6,770 m^2, but it is obviously not completely usable.

The hatch covers are divided into two equal sections and open by sliding along a horizontal plane. The side walkways allow crew passage even when the hatch covers are open, while the walkways between the hatches are occupied by mechanical devices and are not considered as usable for PV panel installation. In this situation, two possible configurations for the installation of PV panels on board can be envisioned: the first involves installing PV panels exclusively on the hatch covers (either including or excluding the cover used as helipad, marked with the letter H); the second involves installing PV panels, in addition to those on the hatch covers, also on the side walkways, while still ensuring free passage for the crew.

It is assumed that the entire surface of the hatch covers and about 80% of the width of each half-hatch cover on the side walkways can be utilised.

Of the seven hatch covers on board, five have the same dimensions, measuring 17.3 m x 15 m; the remaining two have dimensions of 15.57 m x 15 m and 14.7 m x 12.8 m, respectively. Under these conditions, the possible configurations, and the respective areas available for PV panel installation are summarized in Table 9.

Table 9: Configurations for PV installations and related available areas.

Configuration	Description	Available area [m^2]
“config_1_1”	PV panels installed on both hatch covers (helipad included) and side corridors	3,091

“config_1_2”	PV panels installed only on hatch covers (helipad included)	1,719
“config_2_1”	PV panels installed on both hatch covers (helipad excluded) and side corridors	2,858
“config_2_2”	PV panels installed only on hatch covers (helipad excluded)	1,486

Configurations “config_1_1” and “config_1_2” are illustrated in Figure 21, as an example. It is worth noting that each configuration exhibits its own peculiarities. When adopting “config_1_1”, the solar panels are all in use during normal navigation. Since the cargo hatches are all closed during loading/unloading operations, the cargo hatches split into two parts, This covers the solar panels on the sides, thus, disabling their operativity.

On the other hand, when adopting “config_1_2”, the PV system produces the same power both at sea and in port; in this case power produced at sea is lower than in the previous configuration. Once the available surface on board is evaluated for a given configuration and suitable PV panels are selected, according to the criteria indicated in the following subsection, a dedicated software tool is used to define the maximum installable peak power of the integrated shipboard PV system, as described hereinafter.

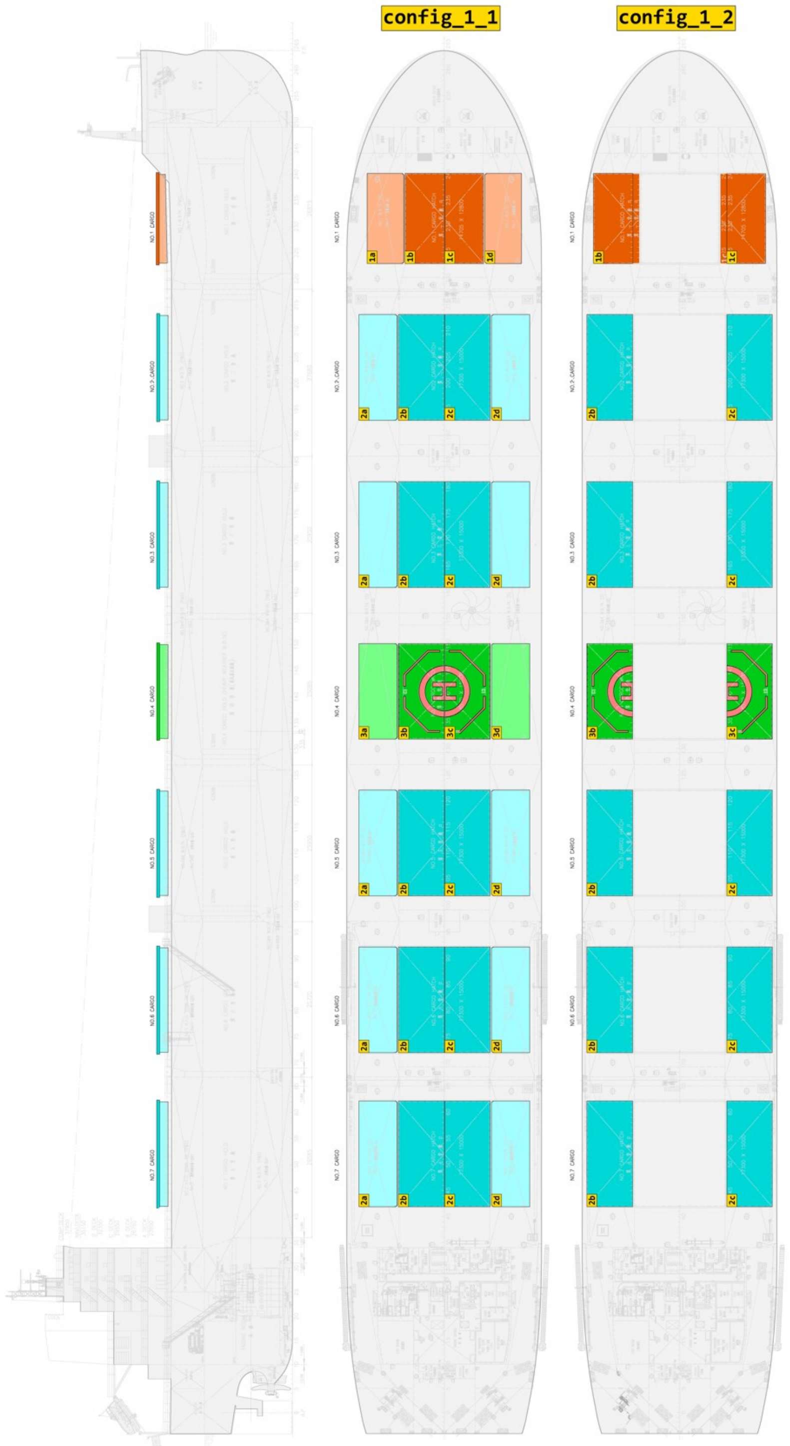

Figure 21: Schemes of configurations “config_1_1” and “config_1_2”

4.2.2 Selection of PV panels

The choice of PV panels potentially installable on the M/V KASTOR ship is done considering the most critical criteria to ensure optimal performance, durability, and reliability of the PV plant in a marine environment. These factors are listed hereinafter:

1. *Efficiency and power output*: it is crucial to choose PV panels with high efficiency, ensuring that they generate maximum power. Monocrystalline silicon panels, known for their higher efficiency, are the preferred choice for the application considered in this study.
2. *Temperature coefficient*: the temperature coefficient of a PV panel is a measure of how its performance changes with temperature. In a marine environment, where temperatures can fluctuate widely, panels with a low temperature coefficient are preferable, as they maintain better performance under heat and cold, preventing significant drops in power production during hot weather or in tropical climates.
3. *Durability and resistance to harsh marine conditions:* the marine environment is tough on equipment due to constant exposure to saltwater, humidity, UV radiation, and temperature fluctuations. It is crucial to choose PV panels that are specifically designed for marine use, such as those made with corrosion-resistant materials and enhanced encapsulation technology. Panels that can withstand saltwater, extreme temperature, and degradation will ensure longevity and reduce maintenance needs.

Rigid PV panels for onboard installation

Rigid PV panels are a common choice for solar installations on ships, offering a range of advantages but also presenting certain challenges. They typically exhibit strong performance in terms of power efficiency (especially the monocrystalline types), and offer durability, longevity, and technology maturity, making them a reliable and proven option for ships that can accommodate their size and weight. As a matter of fact, rigid PV panels are especially suitable for larger vessels, such as the case study ship, where space is not as constrained and where high-power output is essential.

On the other hand, in general, rigid PV panels require flat, stable surfaces for installation, which may not always be available on a ship, especially if the vessel has a curved or irregular structure. While they can be mounted on flat roofs or decks, installation in areas with less ideal surfaces can be challenging and may require additional mounting solutions. This can make installation more complicated and time-consuming compared to flexible panels, which are more adaptable to different shapes and surfaces.

Finally, although rigid PV panels are generally durable, they can be more sensitive to extreme conditions, such as high winds or heavy impacts. For example, they may be more prone to cracking or breaking if subjected to sudden impacts or rough handling during installation or maintenance.

In this study we considered the following two monocrystalline silicon rigid PV panels:

- The PS335M-24/T Premium panel, produced by Phono Solar Technology Co. Ltd
- The PANDA YL265C-30b panel, produced by Yingli Solar

The PS335M-24/T Premium panel is characterised by high efficiency (17.26%), high performance in weak-light conditions, excellent temperature coefficient giving higher yields in the long term, and durability due to the salt mist corrosion resistance guaranteed by the manufacturer. This PV panel model has been already successfully used in maritime applications for the setup of a 427 kW_p solar array installed on a Ro-Ro type marine vessel [89].

The PANDA YL265C-30b panel is manufactured with N-type silicon. This means that energy losses over the years are lower than other modules, due to the use of three electrodes for conduction; it is characterised by high efficiency. In addition, they are distinguished by better performance under conditions of low irradiation and exposure to heat. This panel model has been used for the setup of a 143 kW_p PV system successfully integrated into the electrical power grid of a car and truck carrier [94]. Both rigid PV panels considered are suitable for shipboard integrated PV plants regardless of it being utilized for off-grid applications or connected to the grid.

Flexible PV panels for onboard installation

Flexible PV panels offer several advantages, making them a versatile and appealing option for a variety of applications. One of the primary benefits is their lightweight and flexible nature, which allows for easy transport and installation, especially in non-traditional settings. These panels can be curved or shaped to fit various surfaces, making them ideal for off-grid applications or portable energy solutions. Additionally, their durability is a notable feature, as many flexible panels are designed to withstand harsh environmental conditions like solar radiation, temperature fluctuations, saltwater, and mechanical stress, which enhance their longevity in challenging environments. However, despite their benefits, flexible PV panels do come with some trade-offs.

One of the major drawbacks of flexible PV panels is their typical lower efficiency as compared to traditional rigid panels, meaning that larger surface areas are typically required to generate the same amount of power. This can make them less suitable for situations where space is limited or where high energy output is critical. Furthermore, flexible panels tend to have a higher cost per watt of energy produced due to the specialised materials and manufacturing processes involved in their production. While some flexible panels are designed to be durable, they may still have a shorter lifespan compared to their rigid counterparts, and they may be more vulnerable to physical damage if not handled carefully. In addition, flexible PV panels often struggle in low-light conditions, reducing their performance when exposed to cloudy weather or partial shading. While their aesthetic integration into buildings and ease of installation are major advantages, the overall variety and availability of flexible panels remain more limited than traditional rigid options.

Despite these challenges, the unique attributes of flexible solar technology make it an attractive choice for applications where flexibility, portability, and adaptability are essential, such as in remote locations, on vessels, or for seamless integration into architectural designs.

In the landscape of flexible PV panel manufacturers, Solbian has been identified as a specialised manufacturer in products designed for marine applications. This manufacturer employs an advanced cell encapsulation technique enabling the realisation of solar panels with varying power and features.

The SB (SunBender) series is designed to be compatible with any off-grid installation and is a standard product. It exhibits high efficiency (minimum declared efficiency: 24%) and low temperature coefficient. Moreover, using cells made with a solid copper base, PV panels belonging to SB series are significantly resistant to cracks and corrosion [95].

The SP series utilises back-contact monocrystalline silicon cells, capable of converting over 25% of sunlight into electricity, combined with the encapsulating materials that make panels lightweight and flexible. Designed for extreme conditions, the flexible PV modules can be used in harsh environments and withstand mechanical stress, such as in extreme ocean races. They combine high efficiency with durability against temperature changes, fog, saltwater, solar radiation, and impacts (they are walkable), therefore they are ideal for shipboard integration. The above-described modules are made with specialized techno-polymers, and the technology is patented [95]. Figure 22 shows the appearance of this type of panel installed on a recreational boat.

With large surfaces available on the M/V KASTOR ship, we decided to focus on the panels from the SB and SP series with the highest nominal power, specifically the SB 47 and SP 44 panels.

Table 10 summarises the nominal data of the rigid and flexible PV panels considered in this study.

Figure 22: Flexible PV panels installed on a recreational boat.

Table 10: Nominal data of the selected PV panels

Panel Vendor	**Phono Solar Techn.**	**Yingli Solar**	**Solbian**	
Panel Model	Premium PS335M-24/T	PANDAYL265C-30b	SB 47	SP 44
Panel Current, at Max Power STC (I_{mpp}) [A]	8.72	8.55	5.7	5.6
Panel Current, at short circuit (I_{sc}) [A]	9.04	8.93	6	6
Panel Energy Management	MPPT	MPPT	MPPT	MPTT
Panel length [m]	1.956	1.65	1.054	1.49
Panel width [m]	0.942	0.99	0.8	0.546
Panel thick [m]	0.04	0.005	0.0015	0.002
Panel Voltage, at Max Power STC (V_{mpp}) [V]	38.4	31	28.8	26.8
Panel Voltage, at Open Circuit STC (V_{oc}) [V]	47.2	39	34.1	32
Panel Power (W_p) [W]	335	256	164	150
Cell Efficiency (%)	17.26	16.2	24.4	25.5
Cell Number Tot	60	60	47	44
Cell Technology	Monocrystalline	Monocrystalline	Monocrystalline	Monocrystalline

General considerations on the tilt angle of the PV panels

The tilt angle refers to the angle at which PV panels are positioned with respect to the surface of installation, typically adjusted to capture the most sunlight throughout the day.

The tilt angle significantly affects PV production. In PV panels for land-based applications, the tilt angle is typically set to maximise exposure to sunlight based on the location's latitude and seasonal variations. When the tilt angle is aligned to optimise sunlight capture, the panels generate the most electricity. As the tilt angle increases beyond the optimal setting, the energy yield generally decreases. In cases where the tilt angle is adjusted too high or too low, the cost-to -benefit ratio of installing PV systems may suffer, as more panels or larger systems might be needed to compensate for the lower efficiency.

In many real-world applications, such as in buildings or ships, fixing the tilt angle is the preferred solution due to space or structural constraints, as shown in Figure 23. In such cases, finding the optimal permanent tilt angle becomes crucial to maximising energy production while minimising the costs associated with inefficient configurations.

For a moving platform such as a vessel, anyway, fixing the optimal tilt angle is nontrivial. A study dedicated to defining the optimal tilt angle of a PV array installed on ships revealed that highest amount of produced power is observed when PV panels are installed on a horizontal surface with a loss of about 60% when the tilt angle is set to 45° [96]. This occurs also because of the variability in the angle of incidence between the panels and solar radiation due to ship fluctuations in the sea during navigation, caused by the ship movement along its route but also by roll, pitch and yaw. On such a basis, in this study we only consider installing the PV panels horizontally on the identified available surfaces of the ship.

Figure 23: PV panels installed on a ship according to different tilt angles [96].

4.2.3 Development of a configuration tool for defining the installable PV peak power on-board

To define the peak power of a PV array installed on the M/V KASTOR ship a dedicated software tool has been developed. The software tool has been designed using MATLAB programming and is referred in the following as “R55” configurator. It uses the geometric and electrical characteristics of the ship and the PV panels to define the geometric and electrical configuration of the PV array through which the maximum power installable on board is obtained.

The flow chart in Figure 24 provides a view of the logic on which the “R55” configurator is based and highlights the different levels (geometric and electrical) on which it operates to define the final configuration and derive the corresponding peak power.

The “R55” configurator presents: a table (rapidly extensible) with the rating data of the selected solar panels, various navigation configurations, and an automated algorithm to calculate the best geometrical configuration and series/parallel arrangement of the solar panels to optimise the installed power. From a geometric standpoint, the configurator evaluates the two possible orientations of PV panels with respect to the longitudinal axis of the ship. Both cases of the longest side of the panel parallel and perpendicular to the longitudinal axis of the ship are considered when choosing the arrangement that maximises the number of installable panels.

A table (rapidly extensible) with rating data of batteries can be easily added to the configurator for assessing the footprint of storage systems associated with the PV generator. In our case study, the data related to PV panels described in **Errore. L'origine riferimento non è stata trovata.**10 were given as input to the configurator. The calculation of the installed peak power is performed with reference to PV arrays installed according to the configurations described in sub-section 4.2.1.

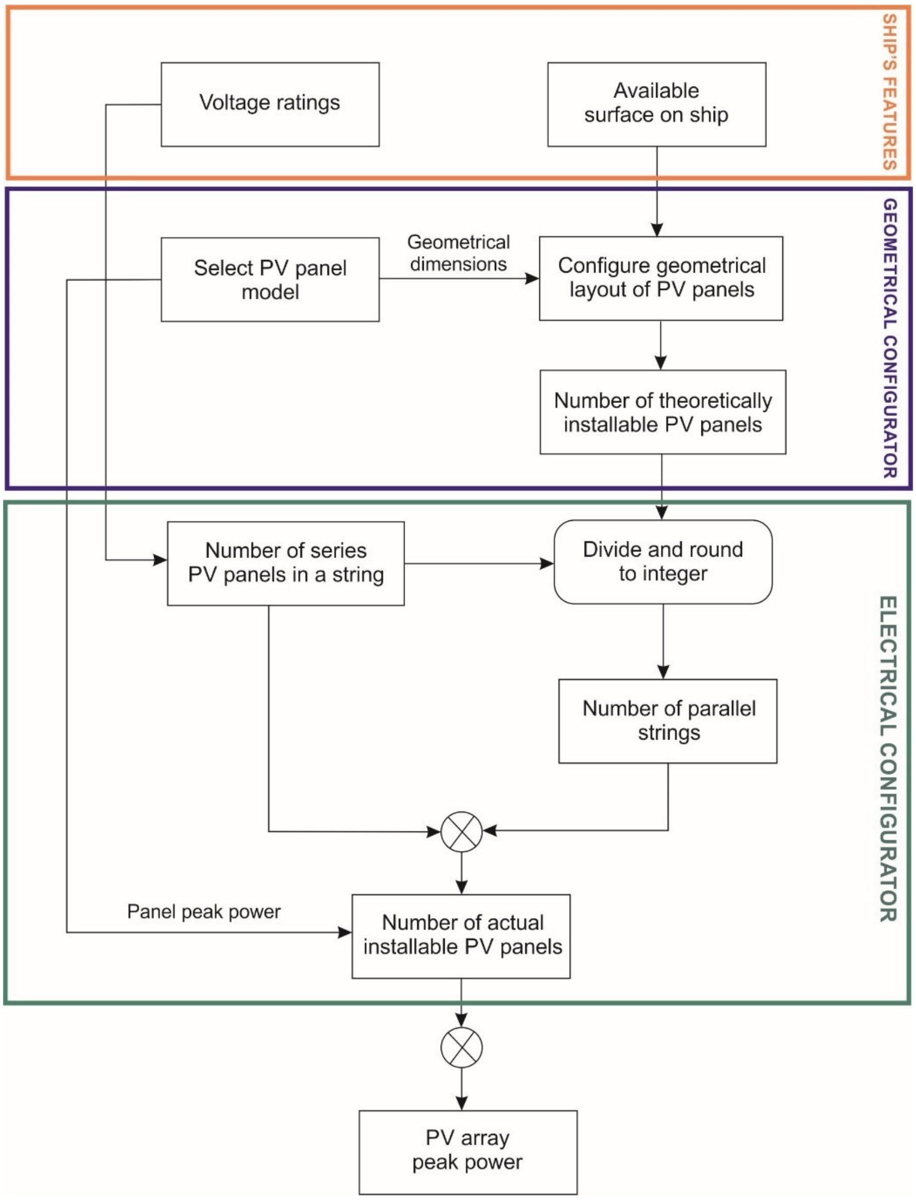

Figure 24: Flow chart describing operation of "R55" configurator.

The area of the surface available on the ship was quantified according to the values obtained for the configurations described in Table 9. The PV system voltage ratings were chosen as per an assumed grid-connected system, thus considering the voltage at the ship's main switchboard, which is 440V AC.

The results obtained for the four configurations described in Table 9, including relevant information like the number of maximum installable PV panels, the electrical layout of the array, and the maximum installable power, are synthesised in Figures Figure 25 and Figure 26.

```
# Vendor,Model,Power,Efficiency,Size,VoltageBar            Area:   3091.16 (m2)         1719.27 (m2)
                                                                  ____________         ____________
1 Premium PS335M-24/T 335W eff:17.26% 1.956m•0.992m Vb:500V      /   cfg_11     \       /   cfg_12     \
  CONFIG-------------    -----11 ------12                       /                \     /                \
  Cargo:TotArea (m2)      3091.16  1719.27                     |  35  42  42  35  |   |  42          42  |
  Cargo:TotPower (kW)      533.53   296.75                     |  51  56  56  51  |   |  56          56  |
  Cargo:TotPanels            1412      742                     |  51  56  56  51  |   |  56          56  |
  PvInst:Series|Prll       13|108    13|57                     |  45  49  49  45  |   |  49          49  |
  PvInst:TotNumber           1404      741                     |  51  56  56  51  |   |  56          56  |
  PvInst:TotPower (kW)     470.34   248.24                     |  51  56  56  51  |   |  56          56  |
  .                                                            |  51  56  56  51  |   |  56          56  |
  .                                                            |__________________|   |__________________|
                                                                  ____________         ____________
2 Yingli YL265C-30b 265W eff:16.2% 1.65m•0.99m Vb:500V           /   cfg_11     \       /   cfg_12     \
  CONFIG-------------    -----11 ------12                       /                \     /                \
  Cargo:TotArea (m2)      3091.16  1719.27                     |  42  48  48  42  |   |  48          48  |
  Cargo:TotPower (kW)      500.77   278.52                     |  60  70  70  60  |   |  70          70  |
  Cargo:TotPanels            1714      922                     |  60  70  70  60  |   |  70          70  |
  PvInst:Series|Prll       16|107    16|57                     |  54  63  63  54  |   |  63          63  |
  PvInst:TotNumber           1712      912                     |  60  70  70  60  |   |  70          70  |
  PvInst:TotPower (kW)     453.68   241.68                     |  60  70  70  60  |   |  70          70  |
  .                                                            |  60  70  70  60  |   |  70          70  |
  .                                                            |__________________|   |__________________|
                                                                  ____________         ____________
3 Solbian SB-47 164W eff:24.4% 1.054m•0.8m Vb:500V               /   cfg_11     \       /   cfg_12     \
  CONFIG-------------    -----11 ------12                       /                \     /                \
  Cargo:TotArea (m2)      3091.16  1719.27                     |  78 108 108  78  |   | 108         108  |
  Cargo:TotPower (kW)      754.24   419.50                     | 112 147 147 112  |   | 147         147  |
  Cargo:TotPanels            3424     1952                     | 112 147 147 112  |   | 147         147  |
  PvInst:Series|Prll       17|201   17|114                     |  98 133 133  98  |   | 133         133  |
  PvInst:TotNumber           3417     1938                     | 112 147 147 112  |   | 147         147  |
  PvInst:TotPower (kW)     560.39   317.83                     | 112 147 147 112  |   | 147         147  |
  .                                                            | 112 147 147 112  |   | 147         147  |
  .                                                            |__________________|   |__________________|
                                                                  ____________         ____________
4 Solbian SP-44 150W eff:25.5% 1.49m•0.54m Vb:500V               /   cfg_11     \       /   cfg_12     \
  CONFIG-------------    -----11 ------12                       /                \     /                \
  Cargo:TotArea (m2)      3091.16  1719.27                     |  81 104 104  81  |   | 104         104  |
  Cargo:TotPower (kW)      788.25   438.41                     | 124 155 155 124  |   | 155         155  |
  Cargo:TotPanels            3664     2038                     | 124 155 155 124  |   | 155         155  |
  PvInst:Series|Prll       18|203   18|113                     | 112 140 140 112  |   | 140         140  |
  PvInst:TotNumber           3664     2038                     | 124 155 155 124  |   | 155         155  |
  PvInst:TotPower (kW)     548.10   305.10                     | 124 155 155 124  |   | 155         155  |
  .                                                            | 124 155 155 124  |   | 155         155  |
  .                                                            |__________________|   |__________________|
```

Figure 25: “R55” configurator output (for “config_1_1” and “config_1_2”)

```
# Vendor,Model,Power,Efficiency,Size,VoltageBar

1 Premium PS335M-24/T 335W eff:17.26% 1.956m•0.992m ShipVb:500V
  CONFIG-------------   ------21 ------22
  Cargo:TotArea (m2)     2857.61  1485.72
  Cargo:TotPower (kW)     493.22   256.44
  Cargo:TotPanels           1314      644
  PvInst:Series|Prll      13|101    13|49
  PvInst:TotNumber          1313      637
  PvInst:TotPower (kW)    439.86   213.40
  .
  .
```

```
   _____________       _____________
  /   cfg_21    \     /   cfg_22    \
 /               \   /               \
  35  42  42  35      42          42
  51  56  56  51      56          56
  51  56  56  51      56          56
  45          45
  51  56  56  51      56          56
  51  56  56  51      56          56
  51  56  56  51      56          56
```

```
2 Yingli YL265C-30b 265W eff:16.2% 1.65m•0.99m ShipVb:500V
  CONFIG-------------   ------21 ------22
  Cargo:TotArea (m2)     2857.61  1485.72
  Cargo:TotPower (kW)     462.93   240.69
  Cargo:TotPanels           1588      796
  PvInst:Series|Prll       16|99    16|49
  PvInst:TotNumber          1584      784
  PvInst:TotPower (kW)    419.76   207.76
  .
  .
```

```
   _____________       _____________
  /   cfg_21    \     /   cfg_22    \
 /               \   /               \
  42  48  48  42      48          48
  60  70  70  60      70          70
  60  70  70  60      70          70
  54          54
  60  70  70  60      70          70
  60  70  70  60      70          70
  60  70  70  60      70          70
```

```
2 Solbian SB-47 164W eff:24.4% 1.054m•0.8m ShipVb:500V
  CONFIG-------------   ------21 ------22
  Cargo:TotArea (m2)     2857.61  1485.72
  Cargo:TotPower (kW)     697.26   362.52
  Cargo:TotPanels           3158     1686
  PvInst:Series|Prll      17|185    17|99
  PvInst:TotNumber          3145     1683
  PvInst:TotPower (kW)    515.78   276.01
  .
  .
```

```
   _____________       _____________
  /   cfg_21    \     /   cfg_22    \
 /               \   /               \
  78 108 108  78     108         108
 112 147 147 112     147         147
 112 147 147 112     147         147
  98          98
 112 147 147 112     147         147
 112 147 147 112     147         147
 112 147 147 112     147         147
```

```
4 Solbian SP-44 150W eff:25.5% 1.49m•0.54m Vb:500V
  CONFIG-------------   ------21 ------22
  Cargo:TotArea (m2)     2857.61  1485.72
  Cargo:TotPower (kW)     728.69   378.86
  Cargo:TotPanels           3384     1758
  PvInst:Series|Prll      18|188    18|97
  PvInst:TotNumber          3384     1746
  PvInst:TotPower (kW)    507.60   261.90
  .
  .
```

```
   _____________       _____________
  /   cfg_21    \     /   cfg_22    \
 /               \   /               \
  81 104 104  81     104         104
 124 155 155 124     155         155
 124 155 155 124     155         155
 112         112
 124 155 155 124     155         155
 124 155 155 124     155         155
 124 155 155 124     155         155
```

Figure 26: “R55” configurator output (for “config_2_1” and “config_2_2”)

The results illustrated in Figure 25: “R55” configurator output (for “config_1_1” and “config_1_2”)show that, depending on the chosen PV panel model, the maximum installable PV power ranges from about 454 kW to about 560 kW for the configuration “config_1_1”. The corresponding power ranges from about 242 kW to about 318 kW for the configuration “config_1_2”. Similarly, from the results shown in Figure 26: “R55” configurator output (for “config_2_1” and “config_2_2”) it is observed that the maximum installable PV power ranges from about 420 kW to about 516 kW for configuration “config_2_1” and from about 208 kW to about 276 kW for configuration “config_2_2.” In any case, the obtained values highlight the potential of a PV plant installed on the ship to provide a non-negligible contribution to the generation of auxiliary power and encourages a deeper analysis of the costs and benefits of this electrical retrofitting solution.

4.2.4 Considerations on the BOP

The BOP in a PV system refers to all the supporting components and infrastructure required for the proper operation of the system, excluding the solar panels themselves. BOP includes items like inverters, transformers, wiring, switchgear, mounting structures, electrical protection systems, energy storage (batteries) and other auxiliary equipment necessary for the generation, conversion, storage and distribution of electricity.

The design, installation and maintenance of the BOP components can significantly impact the overall cost of a PV system. While the solar panels are often the most expensive part, the BOP can account for a significant portion of the total cost. However, investing in high-quality BOP infrastructure can lead to better performance, lower operational costs, and increased energy savings over the lifetime of the system.

The most relevant components from an electrical standpoint are undoubtedly the energy storage systems (ESSs), typically relying on batteries, and the power electronic converters for interfacing the PV source with the load or the onboard.

The intermittency of power output from the PV system and its dependence on location, shipping routes and time zones, makes the use of an ESS essential, even in grid-connected shipboard PV systems, to regulate any power surplus or shortfall. This implies an additional capital cost, weight and availability of suitable spaces on board. A more in-depth discussion of battery sizing in relation to the type of PV array operation in the ship, namely off-grid or grid-connected, power system is developed in deliverable D6.3.

The downward trend in the capital costs of PV modules and batteries registered in the last decades has led to an increased importance of some costs related to BOP. As an example, according to [97], PV inverters contribute around 8-12% of the overall lifetime cost of a PV plant. The choice and sizing of the converters used to interface the PV system to the on-board load/grid is discussed in deliverable D6.3 along with an indication of some commercial converters suitable for the purpose.

Notwithstanding the relevant capital cost of an on-board PV system, a recent techno-economic analysis of a ship-PV grid-connected power system on a car/truck carrier, operating on different routes, demonstrated the implemented solution with a high financial feasibility, in addition to large environmental benefits [98]. This result also encourages pursuing the use of onboard PV generators to meet the efficiency and sustainability requirements set by regulatory bodies in the maritime sector.

4.2.5 Challenges in Evaluating and Managing PV Power Generation on Board

Key challenges for a wider adoption of PV systems on board include:

- Bridging the gap between the installed power and the actual generation,
- Effectively managing onboard power balance.

With regards to the first challenge, the specificity of shipboard PV integration related to the fact that the ship is a moving platform should be noted. Indeed, the shipboard PV plants are in general more prone to partial shading than land-based installations. Therefore, the use of effective maximum power point tracking (MPPT) techniques, such as distributed MPPT (D-MPPT) and static/dynamic reconfiguration strategies, are promising in this technical area to fill the gap between the installed power and the actual generation[99].

As for the second aspect, the accurate PV power prediction is essential to properly handle power balance and management on board, considering the uncertainty and stochastic volatility, typical of renewable sources. By this standpoint, accurate calculation of PV power (P_{PV}) according to Osterwald's method, as in Equation (16), requires an effective forecasting of solar radiation G [100].

$$P_{PV}=\eta_{PV} \times S \times G \times (1-0.005(T_{cell}-25)) \times \eta_{PC} \quad (16)$$

In Equation (16) η_{PV} and η_{PC} are the efficiencies of the PV field and the power converter interfacing the power source with the loads or the power grid. S is the surface of the PV field and T_{cell} is the PV cell temperature in Celsius degrees, obtained using Equation (17):

$$T_{cell}=T_e+\left(\frac{NOCT-20}{800}\right) \times G \quad (17)$$

where T_e is the ambient temperature, NOCT is the operating cell temperature under G=800 W/m^2, T_e= 20 °C and wind speed is taken to be 1 m/s.

It is crucial to observe that the PV forecasting task in vessels is much more challenging than in land-based applications. Indeed, fluctuations caused by weather variations and the motion of the ship increases the uncertainty of PV power output. Therefore, accurate PV forecasting in ships implies spatial-temporal statistical or data-based modelling, as described in Lan, et al. [101] with reference to the day-ahead horizon and a given navigation route.

The use of machine and deep learning approaches, also combined into hybrid and ensemble formulations, is worth considering as a promising method for accurate prediction of shipboard PV generation.

4.2.6 Outline of possible improvements from the synergistic use of various retrofitting solutions including PV

PV generation, used as an auxiliary power source on a ship like the one under study, can be envisioned as an electrical retrofitting measure that can be easily combined with others. Among these measures, the use of shaft generators, possibly supported by batteries, is relevant to the project, since both PV and shaft generators are mature technologies which fit very well with retrofitting concepts. Furthermore, both these solutions enable measurable improvements in design energy efficiency indices established by international regulatory bodies. In detail, the attained EEXI formula [102]includes a term specifically referring to the presence of shaft motor/generator solutions on board. At the same time, PV cells' impact on EEXI is formulated in IMO document MEPC.1/Circ.896 [103] where such a solution is explicitly contemplated as an efficiency-oriented technology implying a saving of auxiliary engine power. This is shown in Figure 27: Classification of energy efficiency technologies according to IMO MEPC.1/CIRC.896 [103], where f_{eff} stands for the availability factor of each innovative energy efficiency technology. Based on these considerations, once the power provided by the above-mentioned electrification technologies has been quantified, the contribution of the same technologies to EEXI reduction can be directly calculated.

The integration of PV panels and shaft generators on board ships represents a forward-thinking approach to enhancing energy efficiency, reducing operational costs and minimising environmental impact.

PVs, as already evidenced, offer a renewable and clean power source that can reduce reliance on traditional fossil fuels. By providing supplementary power for auxiliary systems, PV panels help lower fuel consumption. This not only cuts operational costs but also decreases GHG emissions, supporting the maritime industry's transition towards greener operations and compliance with international environmental regulations such as the IMO's decarbonisation targets. A discussion on the issues related to PV integration on the shipboard electrical microgrid as well as the quantitative assessment of PV use on the ship efficiency design indices are provided in D6.3.

Innovative Energy Efficiency Technologies				
Reduction of Main Engine Power			Reduction of Auxiliary Power	
Category A	*Category B-1*	*Category B-2*	*Category C-1*	*Category C-2*
Cannot be separated from overall performance of the vessel	Can be treated separately from the overall performance of the vessel		Effective at all time	Depending on ambient environment
	$f_{eff}=1$	$f_{eff}<1$	$f_{eff}=1$	$f_{eff}<1$
– low friction coating – bare optimization – rudder resistance – propeller design	– hull air lubrication system (air cavity via air injection to reduce ship resistance) (can be switched off)	– wind assistance (sails, Flettner-Rotors, kites)	– waste heat recovery system (exhaust gas heat recovery and conversion to electric power)	– photovoltaic cells

Figure 27: Classification of energy efficiency technologies according to IMO MEPC.1/CIRC.896 [103]

Shaft generators, in contrast, have been framed as a solution playing a key role in converting mechanical energy from the ship's M/E into electricity. They ensure a stable and efficient power supply for onboard systems, particularly during navigation, while also allowing the need for additional auxiliary engines under certain conditions. When paired with energy storage solutions, such as batteries, shaft generators can further optimise energy use by managing load fluctuations and storing excess power for later use.

The combination of PV panels and shaft generators in a retrofitting perspective is expected therefore, to create a synergistic effect from the standpoint of energy efficiency and environmental friendliness of ships.

5 Conclusion

This report presents a comprehensive analysis of retrofitting solutions designed to achieve a 55% reduction in greenhouse gas emissions from maritime operations by 2030. It highlights the potential of integrating advanced technologies, such as FCs, batteries, WHRS, PTO/PTI and PV to significantly enhance energy efficiency in ship electrification operations. By leveraging these technologies, vessels can optimise their energy management, reduce fuel consumption, and lower their environmental impact. The report underscores the importance of customising solutions to fit the specific operational profiles of different ship types, ensuring compliance with stringent environmental regulations while maintaining operational viability.

The findings indicate that hybrid configurations incorporating these innovative systems can lead to substantial improvements in operational performance and sustainability. As the maritime industry faces increasing pressure to decarbonise, the adoption of these retrofitting technologies is essential. By transitioning to renewable energy sources and implementing zero-carbon solutions, the industry can significantly mitigate its environmental footprint. Ultimately, the successful integration of these advancements will not only contribute to global decarbonisation targets but also position the maritime sector as a leader in sustainable practices, fostering a cleaner and more efficient future for marine transportation.

Future research should focus on the design and optimisation of combined systems that integrate introduced technologies in the ship electrification plant. This holistic approach will allow for a more effective synergy among these technologies, enhancing overall energy efficiency and performance in the plant. Comprehensive field studies are needed to evaluate the long-term reliability and operational effectiveness of these integrated systems under diverse conditions, ultimately identifying best practices for the case study vessel.

In addition to performance optimisation, future studies should incorporate detailed investigations into the environmental impacts of these combined systems. This includes assessing reductions in GHG emissions, particulate matter, and other pollutants resulting from the implementation of these technologies in various maritime contexts. Furthermore, design and size optimisation of the systems concerning the vessel's load profile is crucial.

Safety considerations must also be prioritised; research efforts should analyse how different load conditions affect the performance and efficiency of integrated solutions, enabling the design of systems that are not only effective but also safe and tailored to the specific energy demands of the ship. Collaborative efforts among industry stakeholders, regulatory bodies and research institutions will be essential to develop standardised guidelines that facilitate the widespread adoption and optimisation of these innovative retrofitting solutions, paving the way for a more sustainable maritime future.

References

[1] M. Kamran *et al.*, "Assessment of greenhouse gases emissions, global warming potential and net ecosystem economic benefits from wheat field with reduced irrigation and nitrogen management in an arid region of China," *Agriculture, Ecosystems & Environment,* vol. 341, p. 108197, 2023/01/01/ 2023, doi: https://doi.org/10.1016/j.agee.2022.108197.

[2] A. Mikhaylov, N. Moiseev, K. Aleshin, and T. Burkhardt, "Global climate change and greenhouse effect," *Entrepreneurship and Sustainability Issues,* vol. 7, no. 4, pp. 2897-2913, 2020, doi: 10.9770/jesi.2020.7.4(21).

[3] I. S. Seddiek and N. R. Ammar, "Technical and eco-environmental analysis of blue/green ammonia-fueled RO/RO ships," (in English), *Transportation Research Part D: Transport and Environment,* vol. 114, JAN 2023, Art no. 103547, doi: 10.1016/j.trd.2022.103547.

[4] UNCTAD. "Review of Maritime Transport 2023. Towards a green and just transition." https://unctad.org/publication/review-maritime-transport-2023 (accessed 03/05/2024, 2024).

[5] H. Bach and T. Hansen, "IMO off course for decarbonisation of shipping? Three challenges for stricter policy," *Marine Policy,* vol. 147, p. 105379, 2023/01/01/ 2023, doi: https://doi.org/10.1016/j.marpol.2022.105379.

[6] L. Styhre, H. Winnes, J. Black, J. Lee, and H. Le-Griffin, "Greenhouse gas emissions from ships in ports – Case studies in four continents," *Transportation Research Part D: Transport and Environment,* vol. 54, pp. 212-224, 2017/07/01/ 2017, doi: https://doi.org/10.1016/j.trd.2017.04.033.

[7] H. Tu, Z. Liu, and Y. Zhang, "Study on Cost-Effective Performance of Alternative Fuels and Energy Efficiency Measures for Shipping Decarbonization," *Journal of Marine Science and Engineering,* vol. 12, no. 5, 2024, doi: 10.3390/jmse12050743.

[8] E. Ejder, S. Dinçer, and Y. Arslanoglu, "Decarbonization strategies in the maritime industry: An analysis of dual-fuel engine performance and the carbon intensity indicator," *Renewable and Sustainable Energy Reviews,* vol. 200, p. 114587, 2024/08/01/ 2024, doi: https://doi.org/10.1016/j.rser.2024.114587.

[9] M. Bayraktar and O. Yuksel, "A scenario-based assessment of the energy efficiency existing ship index (EEXI) and carbon intensity indicator (CII) regulations," *Ocean Engineering,* vol. 278, 2023, doi: 10.1016/j.oceaneng.2023.114295.

[10] O. Konur, O. Yuksel, S. Aykut Korkmaz, C. Ozgur Colpan, O. Y. Saatcioglu, and B. Koseoglu, "Operation-dependent exergetic sustainability assessment and environmental analysis on a large tanker ship utilizing Organic Rankine cycle system," *Energy,* vol. 262, 2023, doi: 10.1016/j.energy.2022.125477.

[11] O. Yuksel and B. Koseoglu, "Numerical simulation of the hybrid ship power distribution system and an analysis of its emission reduction potential," *Ships and Offshore Structures,* vol. 18, no. 1, pp. 78-94, 2023, doi: 10.1080/17445302.2022.2028435.

[12] J. Markowski and I. Pielecha, "The potential of fuel cells as a drive source of maritime transport," *IOP Conference Series : Earth and Environmental Science,* vol. 214, pp. 012019-undefined, 2019, doi: 10.1088/1755-1315/214/1/012019.

[13] P. Zhu *et al.*, "The dynamic response of solid oxide fuel cell fueled by syngas during the operating condition variations," *Applied Energy,* vol. 349, p. 121655, 2023/11/01/ 2023, doi: https://doi.org/10.1016/j.apenergy.2023.121655.

[14] O. Yuksel, "A comprehensive feasibility analysis of dual-fuel engines and solid oxide fuel cells on a tanker ship considering environmental, economic, and regulation aspects," *Sustainable Production and Consumption,* vol. 42, pp. 106-124, 2023, doi: 10.1016/j.spc.2023.09.012.

[15] E. Vehkala, "Fuel Cell Waste Heat Recovery in Marine Applications," Master's, Environmental and Energy Engineering, Tampere University, Tampere, 2023. [Online].

Available: https://trepo.tuni.fi/bitstream/handle/10024/149854/VehkalaEveliina.pdf?sequence=2
[16] M. Turco, A. Ausiello, and L. Micoli, "Fuel Cells Operating and Structural Features of MCFCs and SOFCs," in *Treatment of Biogas for Feeding High Temperature Fuel Cells: Removal of Harmful Compounds by Adsorption Processes*, M. Turco, A. Ausiello, and L. Micoli Eds. Cham: Springer International Publishing, 2016, pp. 31-76.
[17] A. Sohani *et al.*, "Application based multi-objective performance optimization of a proton exchange membrane fuel cell," *Journal of Cleaner Production,* vol. 252, p. 119567, 2020/04/10/ 2020, doi: https://doi.org/10.1016/j.jclepro.2019.119567.
[18] HFTO. "Comparison of Fuel Cell Technologies." https://www.energy.gov/eere/fuelcells/comparison-fuel-cell-technologies (accessed 02/07/2024, 2024).
[19] S. A. Korkmaz, K. E. Erginer, O. Yuksel, O. Konur, and C. O. Colpan, "Environmental and economic analyses of fuel cell and battery-based hybrid systems utilized as auxiliary power units on a chemical tanker vessel," *International Journal of Hydrogen Energy,* vol. 48, no. 60, pp. 23279-23295, 2023, doi: 10.1016/j.ijhydene.2023.01.320.
[20] M. Luna, G. La Tona, A. Accetta, M. Pucci, A. Pietra, and M. C. Di Piazza, "Optimal Management of Battery and Fuel Cell-Based Decentralized Generation in DC Shipboard Microgrids," *Energies,* vol. 16, no. 4, 2023, doi: 10.3390/en16041682.
[21] H. Seyfi, D. Hitchmough, M. Armin, and E. Blanco-Davis, "A Study on the Viability of Fuel Cells as an Alternative to Diesel Fuel Generators on Ships," *Journal of Marine Science and Engineering,* vol. 11, no. 8, 2023, doi: 10.3390/jmse11081489.
[22] R. Fisher *et al.*, "Innovative waste heat valorisation technologies for zero-carbon ships − A review," *Applied Thermal Engineering,* vol. 253, p. 123740, 2024/09/15/ 2024, doi: https://doi.org/10.1016/j.applthermaleng.2024.123740.
[23] O. Konur, O. Yuksel, S. A. Korkmaz, C. O. Colpan, O. Y. Saatcioglu, and I. Muslu, "Thermal design and analysis of an organic rankine cycle system utilizing the main engine and cargo oil pump turbine based waste heats in a large tanker ship," *Journal of Cleaner Production,* vol. 368, 2022, doi: 10.1016/j.jclepro.2022.133230.
[24] D. V. Singh and E. Pedersen, "A review of waste heat recovery technologies for maritime applications," *Energy Conversion and Management,* vol. 111, pp. 315-328, 2016/03/01/ 2016, doi: https://doi.org/10.1016/j.enconman.2015.12.073.
[25] F. Gao, A. H. Brodtkorb, M. Zadeh, and S. M. Mo, "Power management and optimization of marine hybrid propulsion systems: A combinator surface methodology," *Ocean Engineering,* vol. 309, p. 118354, 2024/10/01/ 2024, doi: https://doi.org/10.1016/j.oceaneng.2024.118354.
[26] M. Altosole, F. Balsamo, A. Bove, U. Campora, N. Ianniello, and L. Vitiello, "Progress in Marine Hybrid Propulsion Drive Systems," in *2023 IEEE International Conference on Electrical Systems for Aircraft, Railway, Ship Propulsion and Road Vehicles & International Transportation Electrification Conference (ESARS-ITEC)*, 29-31 March 2023 2023, pp. 1-6, doi: 10.1109/ESARS-ITEC57127.2023.10114887.
[27] Z. Zapałowicz and W. Zeńczak, "The possibilities to improve ship's energy efficiency through the application of PV installation including cooled modules," *Renewable and Sustainable Energy Reviews,* vol. 143, p. 110964, 2021/06/01/ 2021, doi: https://doi.org/10.1016/j.rser.2021.110964.
[28] M. Paulson and D. Chacko, "Marine photovoltaics: A review of research and developments, challenges and future trends," *Int. J. Sci. Technol. Res,* vol. 8, pp. 1479-1488, 2019.
[29] M. Buitendijk. "How to get an existing bulk carrier to meet EEXI and CII." https://swzmaritime.nl/news/2023/01/30/how-to-get-an-existing-bulk-carrier-to-meet-eexi-and-cii/ (accessed 24/01/2025, 2025).

[30] A. Habibic. "Industry's first: Wärtsilä installs hybrid solution onboard bulk carrier." https://www.offshore-energy.biz/industrys-first-wartsila-installs-hybrid-solution-onboard-bulk-carrier/ (accessed 24/01/2025, 2025).

[31] WHISPER. "About WHISPER." https://www.whisperenergy.eu/about-whisper/ (accessed 24/01/2025, 2024).

[32] ENGIMMONIA. "Documentation." **https://www.engimmonia.eu/documentation/** (accessed 24/01/2025, 2025).

[33] A. Spiteri *et al.*, "Framework for Safe and Sustainable Shipping Operations," in "RETROFIT SOLUTIONS TO ACHIEVE 55% GHG REDUCTION BY 2030," 2024. [Online]. Available: https://www.retrofit55.eu/wp-content/uploads/2024/10/D1.1__Framework-for-safe-and-sustainable-shipping-operations.pdf

[34] J. Prousalidis *et al.*, "Characterization of the ship systems and Electric Load Analysis (ELA)," in "RETROFIT SOLUTIONS TO ACHIEVE 55% GHG REDUCTION BY 2030," 2024. [Online]. Available: https://www.retrofit55.eu/wp-content/uploads/2024/10/D6.1__Characterization-of-the-ship-systems-and-ELA.pdf

[35] C. O. Peralta P, G. T. T. Vieira, S. Meunier, R. J. Vale, M. B. C. Salles, and B. S. Carmo, "Evaluation of the CO2 Emissions Reduction Potential of Li-ion Batteries in Ship Power Systems," *Energies,* vol. 12, no. 3, 2019, doi: 10.3390/en12030375.

[36] E. Baldasso *et al.*, "Organic Rankine cycle-based waste heat recovery system combined with thermal energy storage for emission-free power generation on ships during harbor stays," *Journal of Cleaner Production,* vol. 271, p. 122394, 2020/10/20/ 2020, doi: https://doi.org/10.1016/j.jclepro.2020.122394.

[37] O. B. Inal, B. Zincir, C. Dere, and J.-F. Charpentier, "Hydrogen Fuel Cell as an Electric Generator: A Case Study for a General Cargo Ship," *Journal of Marine Science and Engineering 2024, Vol. 12, Page 432,* vol. 12, no. 3, pp. 432-432, 2024, doi: 10.3390/JMSE12030432.

[38] S. Mekhilef, R. Saidur, and A. Safari, "Comparative study of different fuel cell technologies," *Renewable and Sustainable Energy Reviews,* vol. 16, no. 1, pp. 981-989, 2012/01/01/ 2012, doi: https://doi.org/10.1016/j.rser.2011.09.020.

[39] L. Giorgi and F. Leccese, "Fuel Cells: Technologies and Applications," *The Open Fuel Cells Journal,* vol. 6, pp. 1-20, 2013, doi: 10.2174/1875932720130719001.

[40] J. W. Patrick, "Handbook of fuel cells. Fundamentals technology and applications: Wolf Vielstich, Arnold Lamm, Hubert A. Gasteiger (Eds.); John Wiley and Sons Ltd, Chichester, England, 2003, Vols 1–4, 449 pages (vol. 1), 783 pages (vol. 2), 1372 pages (vols 3 and 4), ISBN: 0-471-49926-9, £895," *Fuel,* vol. 83, no. 4, p. 623, 2004/03/01/ 2004, doi: https://doi.org/10.1016/j.fuel.2003.09.012.

[41] N. A. A. Qasem and G. A. Q. Abdulrahman, "A Recent Comprehensive Review of Fuel Cells: History, Types, and Applications," *International Journal of Energy Research,* vol. 2024, no. 1, p. 7271748, 2024/01/01 2024, doi: https://doi.org/10.1155/2024/7271748.

[42] X. Li, "Biomass Energy Systems - Fuel Cells," in *Energy Efficiency and Renewable Energy Handbook*, Second ed., D. Y. Goswami and F. Kreith, Eds. Boca Raton: CRC Press, 2016.

[43] D. E. Eapen, S. R. Suseendiran, and R. Rengaswamy, "2 - Phosphoric acid fuel cells," in *Compendium of Hydrogen Energy*, F. Barbir, A. Basile, and T. N. Veziroğlu Eds. Oxford: Woodhead Publishing, 2016, pp. 57-70.

[44] W. Gao, "Performance comparison of a fuel cell-battery hybrid powertrain and a fuel cell-ultracapacitor hybrid powertrain," *IEEE Transactions on Vehicular Technology,* vol. 54, no. 3, pp. 846-855, 2005, doi: 10.1109/TVT.2005.847229.

[45] R. Lan, X. Xu, S. Tao, and J. T. S. Irvine, "A fuel cell operating between room temperature and 250°C based on a new phosphoric acid based composite electrolyte," *Journal of Power*

Sources, vol. 195, no. 20, pp. 6983-6987, 2010/10/15/ 2010, doi: https://doi.org/10.1016/j.jpowsour.2010.04.076.
[46] P. L. Zervas, M. K. Koukou, and N. C. Markatos, "Predicting the effects of process parameters on the performance of phosphoric acid fuel cells using a 3-D numerical approach," *Energy Conversion and Management,* vol. 47, no. 18, pp. 2883-2899, 2006/11/01/ 2006, doi: https://doi.org/10.1016/j.enconman.2006.03.030.
[47] H.-Y. Kwak, H.-S. Lee, J.-S. Jeon, and D. Choi, "Exergetic and Thermoeconomic Analysis of a 200-KW Phosphoric Acid Fuel Cell Plant," 2001. [Online]. Available: https://doi.org/10.1115/IMECE2001/AES-23649.
[48] S. J. Seo, H.-I. Joh, H. T. Kim, and S. H. Moon, "Properties of Pt/C catalyst modified by chemical vapor deposition of Cr as a cathode of phosphoric acid fuel cell," *Electrochimica Acta,* vol. 52, no. 4, pp. 1676-1682, 2006/12/01/ 2006, doi: https://doi.org/10.1016/j.electacta.2006.03.104.
[49] Doosan. "PureCell Model 400." https://www.doosanfuelcellpower.com/download/pdf/catalog/pafc-400kw_en.pdf (accessed 01/05/2021, 2024).
[50] S. Zarabi Golkhatmi, M. I. Asghar, and P. D. Lund, "A review on solid oxide fuel cell durability: Latest progress, mechanisms, and study tools," *Renewable and Sustainable Energy Reviews,* vol. 161, p. 112339, 2022/06/01/ 2022, doi: https://doi.org/10.1016/j.rser.2022.112339.
[51] J. Liu, S.-C. Kim, and K.-Y. Shin, "Feasibility Study and Economic Analysis of a Fuel-Cell-Based CHP System for a Comprehensive Sports Center with an Indoor Swimming Pool," *Energies*, vol. 14, no. 20, doi: 10.3390/en14206625.
[52] N. H. Behling, "Chapter 4 - History of Phosphoric Acid Fuel Cells," in *Fuel Cells*, N. H. Behling Ed.: Elsevier, 2013, pp. 53-135.
[53] J. Ding, P. Wang, S. Ji, H. Wang, V. Linkov, and R. Wang, "N-doped mesoporous FeNx/carbon as ORR and OER bifunctional electrocatalyst for rechargeable zinc-air batteries," *Electrochimica Acta,* vol. 296, pp. 653-661, 2019/02/10/ 2019, doi: https://doi.org/10.1016/j.electacta.2018.11.105.
[54] A. Gong and D. Verstraete, "Fuel cell propulsion in small fixed-wing unmanned aerial vehicles: Current status and research needs," *International Journal of Hydrogen Energy,* vol. 42, no. 33, pp. 21311-21333, 2017/08/17/ 2017, doi: https://doi.org/10.1016/j.ijhydene.2017.06.148.
[55] Q. Wang *et al.*, "Phenylenediamine-Based FeNx/C Catalyst with High Activity for Oxygen Reduction in Acid Medium and Its Active-Site Probing," *Journal of the American Chemical Society,* vol. 136, no. 31, pp. 10882-10885, 2014/08/06 2014, doi: 10.1021/ja505777v.
[56] PowerCellGroup. "Marine System 200." https://powercellgroup.com/product/marine-system-200/ (accessed 01/05/2024, 2024).
[57] Crystec. "Ammonia Cracker for the Generation of Forming Gas." https://www.crystec.com/kllhyame.htm#Hydrogen_PSA (accessed 07/08/2024, 2024).
[58] SMA. "SUNNY CENTRAL STORAGE." https://files.sma.de/assets/275864.pdf (accessed 23/05/2024, 2024).
[59] DOE. "Types of Fuel Cells." https://www.energy.gov/eere/fuelcells/types-fuel-cells (accessed 21/11/2024, 2024).
[60] M. Singh, D. Zappa, and E. Comini, "Solid oxide fuel cell: Decade of progress, future perspectives and challenges," *International Journal of Hydrogen Energy,* vol. 46, no. 54, pp. 27643-27674, 2021/08/05/ 2021, doi: https://doi.org/10.1016/j.ijhydene.2021.06.020.
[61] FuelCellEnergy. "SOLID OXIDE FUEL CELL 250 kW." https://go.fuelcellenergy.com/hubfs/Solid%20Oxide%20Fuel%20Cell%20Spec%20Sheet.pdf (accessed 01/05/2024, 2024).

[62] Z. Abdin, A. Zafaranloo, A. Rafiee, W. Mérida, W. Lipiński, and K. R. Khalilpour, "Hydrogen as an energy vector," *Renewable and Sustainable Energy Reviews,* vol. 120, p. 109620, 2020/03/01/ 2020, doi: https://doi.org/10.1016/j.rser.2019.109620.

[63] Y. Liu, J. Liu, L. Fu, and Q. Wang, "Numerical Study on Effects of Flow Channel Length on Solid Oxide Fuel Cell-Integrated System Performances," *Sustainability*, vol. 16, no. 4, doi: 10.3390/su16041643.

[64] M. Z. Khan, A. Hussain, S.-B. Lee, T.-H. Lim, and R.-H. Song, "Anticipating the lifespan: Predicting the durability of an anode-supported solid oxide fuel cell short stack over 50,000 h," *Progress in Natural Science: Materials International,* 2024/05/28/ 2024, doi: https://doi.org/10.1016/j.pnsc.2024.05.012.

[65] S. Saxena, C. Hendricks, and M. Pecht, "Cycle life testing and modeling of graphite/LiCoO2 cells under different state of charge ranges," *Journal of Power Sources,* vol. 327, pp. 394-400, 2016/09/30/ 2016, doi: https://doi.org/10.1016/j.jpowsour.2016.07.057.

[66] Panasonic. "Specifications for NCR18650GA." https://www.orbtronic.com/content/Datasheet-specs-Sanyo-Panasonic-NCR18650GA-3500mah.pdf (accessed 01/05/2024, 2024).

[67] S. Sepasi, R. Ghorbani, and B. Y. Liaw, "Inline state of health estimation of lithium-ion batteries using state of charge calculation," *Journal of Power Sources,* vol. 299, pp. 246-254, 2015/12/20/ 2015, doi: https://doi.org/10.1016/j.jpowsour.2015.08.091.

[68] E. Ovrum and T. F. Bergh, "Modelling lithium-ion battery hybrid ship crane operation," *Applied Energy,* vol. 152, pp. 162-172, 2015/08/15/ 2015, doi: https://doi.org/10.1016/j.apenergy.2015.01.066.

[69] I. Girgin and C. Ezgi, "Design and thermodynamic and thermoeconomic analysis of an organic Rankine cycle for naval surface ship applications," *Energy Conversion and Management,* vol. 148, pp. 623-634, 2017/09/15/ 2017, doi: https://doi.org/10.1016/j.enconman.2017.06.033.

[70] M. E. Mondejar, J. G. Andreasen, L. Pierobon, U. Larsen, M. Thern, and F. Haglind, "A review of the use of organic Rankine cycle power systems for maritime applications," *Renewable and Sustainable Energy Reviews,* vol. 91, pp. 126-151, 2018/08/01/ 2018, doi: https://doi.org/10.1016/j.rser.2018.03.074.

[71] L. Lyu, A. Kan, W. Chen, Y. Zhang, and B. Fu, "Energy, Exergy and Environmental Analysis of ORC Waste Heat Recovery from Container Ship Exhaust Gases Based on Voyage Cycle," *Journal of Marine Science and Engineering,* vol. 11, no. 10, 2023, doi: 10.3390/jmse11102029.

[72] N. Gültekin and M. Ciniviz, "Examination of the effect of combustion chamber geometry and mixing ratio on engine performance and emissions in a hydrogen-diesel dual-fuel compression-ignition engine," *International Journal of Hydrogen Energy,* vol. 48, no. 7, pp. 2801-2820, 2023/01/22/ 2023, doi: https://doi.org/10.1016/j.ijhydene.2022.10.155.

[73] S. L. Kuzu, L. Bilgili, and A. Kiliç, "Estimation and dispersion analysis of shipping emissions in Bandirma Port, Turkey," *Environment, Development and Sustainability,* vol. 23, no. 7, pp. 10288-10308, 2021/07/01 2021, doi: 10.1007/s10668-020-01057-6.

[74] P. Gilbert, C. Walsh, M. Traut, U. Kesieme, K. Pazouki, and A. Murphy, "Assessment of full life-cycle air emissions of alternative shipping fuels," *Journal of Cleaner Production,* vol. 172, pp. 855-866, 2018/01/20/ 2018, doi: https://doi.org/10.1016/j.jclepro.2017.10.165.

[75] N. Pavlenko, Comer B., Y. Zhou, and N. Clark, "The climate implications of using LNG as a marine fuel," INTERNATIONAL COUNCIL ON CLEAN TRANSPORTATION, 2020. [Online]. Available: https://theicct.org/sites/default/files/publications/Climate_implications_LNG_marinefuel_01282020.pdf

[76] IMO. "2024 GUIDELINES ON LIFE CYCLE GHG INTENSITY OF MARINE FUELS (2024 LCA Guidelines)." https://wwwcdn.imo.org/localresources/en/KnowledgeCentre/IndexofIMOResolutions/MEPCDocuments/MEPC.391(81).pdf (accessed 13/11/2024, 2024).
[77] S. Di Micco, L. Mastropasqua, V. Cigolotti, M. Minutillo, and J. Brouwer, "A framework for the replacement analysis of a hydrogen-based polymer electrolyte membrane fuel cell technology on board ships: A step towards decarbonization in the maritime sector," *Energy Conversion and Management,* vol. 267, p. 115893, 2022/09/01/ 2022, doi: https://doi.org/10.1016/j.enconman.2022.115893.
[78] IEA -PVPS, Trends in PV 2022. 2022
[79] J. Prousalidis, C. Patsios, F. Kanellos, A. Sarigiannidis, N. Tsekouras, and G. Antonopoulos, "Exploiting shaft generators to improve ship efficiency," in *2012 Electrical Systems for Aircraft, Railway and Ship Propulsion*, 16-18 Oct. 2012 2012, pp. 1-6, doi: 10.1109/ESARS.2012.6387443.
[80] A. Sarigiannidis, A. Kladas, E. Chatzinikolaou, and C. Patsios, "High efficiency Shaft Generator drive system design for Ro-Ro trailer-passenger ship application," in *2015 International Conference on Electrical Systems for Aircraft, Railway, Ship Propulsion and Road Vehicles (ESARS)*, 3-5 March 2015 2015, pp. 1-6, doi: 10.1109/ESARS.2015.7101529.
[81] A. G. Sarigiannidis, E. Chatzinikolaou, C. Patsios, and A. G. Kladas, "Shaft Generator System Design and Ship Operation Improvement Involving SFOC Minimization, Electric Grid Conditioning, and Auxiliary Propulsion," *IEEE Transactions on Transportation Electrification,* vol. 2, no. 4, pp. 558-569, 2016, doi: 10.1109/TTE.2016.2614999.
[82] MAN, "MAN B&W S60ME-C8.5-TII, Project Guide, Electronically Controlled Two-stroke Engines," 2018.
[83] N. M. Haegel and S. R. Kurtz, "Global Progress Toward Renewable Electricity: Tracking the Role of Solar (Version 3)," *IEEE Journal of Photovoltaics,* vol. 13, no. 6, pp. 768-776, 2023, doi: 10.1109/JPHOTOV.2023.3309922.
[84] G. L. Tona and M. C. D. Piazza, "ANN-based forecasting of solar irradiation under data clustering: an approach for improved estimation of PV power production," in *2023 IEEE 32nd International Symposium on Industrial Electronics (ISIE)*, 19-21 June 2023 2023, pp. 1-6, doi: 10.1109/ISIE51358.2023.10228061.
[85] O. Yuksel *et al.*, "Optimising the Design of a Hybrid Fuel Cell/Battery and Waste Heat Recovery System for Retrofitting Ship Power Generation," *Energies*, vol. 18, no. 2, doi: 10.3390/en18020288.
[86] V. J. Jimenez, H. Kim, and Z. H. Munim, "A review of ship energy efficiency research and directions towards emission reduction in the maritime industry," *Journal of Cleaner Production,* vol. 366, p. 132888, 2022/09/15/ 2022, doi: https://doi.org/10.1016/j.jclepro.2022.132888.
[87] I. Kobougias, E. Tatakis, and J. Prousalidis, "PV Systems Installed in Marine Vessels: Technologies and Specifications," *Advances in Power Electronics,* vol. 2013, no. 1, p. 831560, 2013/01/01 2013, doi: https://doi.org/10.1155/2013/831560.
[88] DNV. "MARITIME FORECAST TO 2050 EXECUTIVE SUMMARY AND HIGHLIGHTS Energy Transition Outlook 2022." https://www.dnv.com/publications/maritime-forecast-to-2050-2022-edition-235251/ (accessed 23/01/2025, 2025).
[89] Ç. Karatuğ and Y. Durmuşoğlu, "Design of a solar photovoltaic system for a Ro-Ro ship and estimation of performance analysis: A case study," *Solar Energy,* vol. 207, pp. 1259-1268, 2020/09/01/ 2020, doi: https://doi.org/10.1016/j.solener.2020.07.037.
[90] P. Schwager, K. Gehrke, and M. Vehse, "Applicability of Standard Photovoltaic Modules for an Increased Share of Renewable Energies on Board Cruise Ships," in *2021 Sixteenth*

International Conference on Ecological Vehicles and Renewable Energies (EVER), 5-7 May 2021 2021, pp. 1-5, doi: 10.1109/EVER52347.2021.9456658.
[91] J. P. Kirkpatrick, "An investigation of the effectiveness of solar power on Navy surface combatants," Monterey, California: Naval Postgraduate School, 2013.
[92] H. Yin *et al.*, "A Comprehensive Review of Shipboard Power Systems with New Energy Sources," *Energies*, vol. 16, no. 5, doi: 10.3390/en16052307.
[93] R. Zhang and H. Liang, "Application of solar energy in ship power field," in *2022 IEEE Asia-Pacific Conference on Image Processing, Electronics and Computers (IPEC)*, 14-16 April 2022 2022, pp. 1588-1590, doi: 10.1109/IPEC54454.2022.9777324.
[94] Y. Yuan, J. Wang, X. Yan, Q. Li, and T. Long, "A design and experimental investigation of a large-scale solar energy/diesel generator powered hybrid ship," *Energy,* vol. 165, pp. 965-978, 2018/12/15/ 2018, doi: https://doi.org/10.1016/j.energy.2018.09.085.
[95] Solbian. "Power meets experience." (accessed 24/01/2025, 2025).
[96] H. Lan, J. Dai, S. Wen, Y.-Y. Hong, D. C. Yu, and Y. Bai, "Optimal Tilt Angle of Photovoltaic Arrays and Economic Allocation of Energy Storage System on Large Oil Tanker Ship," *Energies*, vol. 8, no. 10, pp. 11515-11530doi: 10.3390/en81011515.
[97] A. Nagarajan, T. Ramanathan, I. Repins, and P. Hacke, "Photovoltaic Inverter Reliability Assessment " National Renewable Energy Laboratory NREL/TP-5D00-74462, 2019. [Online]. Available: https://www.nrel.gov/docs/fy20osti/74462.pdf
[98] Y. Qiu, C. Yuan, J. Tang, and X. Tang, "Techno-economic analysis of PV systems integrated into ship power grid: A case study," *Energy Conversion and Management,* vol. 198, p. 111925, 2019/10/15/ 2019, doi: https://doi.org/10.1016/j.enconman.2019.111925.
[99] A. M. Ajmal, T. Sudhakar Babu, V. K. Ramachandaramurthy, D. Yousri, and J. B. Ekanayake, "Static and dynamic reconfiguration approaches for mitigation of partial shading influence in photovoltaic arrays," *Sustainable Energy Technologies and Assessments,* vol. 40, p. 100738, 2020/08/01/ 2020, doi: https://doi.org/10.1016/j.seta.2020.100738.
[100] C. R. Osterwald, "Translation of device performance measurements to reference conditions," *Solar Cells,* vol. 18, no. 3, pp. 269-279, 1986/09/01/ 1986, doi: https://doi.org/10.1016/0379-6787(86)90126-2.
[101] H. Lan, H. Yin, Y.-Y. Hong, S. Wen, D. C. Yu, and P. Cheng, "Day-ahead spatio-temporal forecasting of solar irradiation along a navigation route," *Applied Energy,* vol. 211, pp. 15-27, 2018/02/01/ 2018, doi: https://doi.org/10.1016/j.apenergy.2017.11.014.
[102] IMO. "2022 GUIDELINES ON THE METHOD OF CALCULATION OF THE ATTAINED ENERGY EFFICIENCY EXISTING SHIP INDEX (EEXI)." https://wwwcdn.imo.org/localresources/en/KnowledgeCentre/IndexofIMOResolutions/MEPCDocuments/MEPC.350(78).pdf (accessed 24/06/2024, 2024).
[103] IMO. "2021 GUIDANCE ON TREATMENT OF INNOVATIVE ENERGY EFFICIENCY TECHNOLOGIES FOR CALCULATION AND VERIFICATION OF THE ATTAINED EEDI AND EEXI." https://wwwcdn.imo.org/localresources/en/OurWork/Environment/Documents/Air%20pollution/MEPC.1-Circ.896.pdf (accessed 24/01/2025, 2025).